

## **Antarctic coastal nanoplankton dynamics revealed by metabarcoding of desalination plant filters: detection of short-term events and implications for routine monitoring**

Matteo Cecchetto<sup>a,b</sup>, Andrea Di Cesare<sup>c</sup>, Ester Eckert<sup>c</sup>, Giulia Fassio<sup>d</sup>, Diego Fontaneto<sup>c</sup>, Isabella Moro<sup>e</sup>, Marco Oliverio<sup>d</sup>, Katia Sciuto<sup>e,f</sup>, Giovanni Tassistro<sup>b</sup>, Luigi Vezzulli<sup>b</sup>, Stefano Schiaparelli<sup>a,b</sup>

<sup>a</sup>Italian National Antarctic Museum (MNA, Section of Genoa), University of Genoa, Genoa, Italy

<sup>b</sup>Department of Earth, Environmental and Life Science (DISTAV), University of Genoa, Genoa, Italy

<sup>c</sup>National Research Council of Italy, Water Research Institute (CNR-IRSA), Verbania Pallanza, Italy

<sup>d</sup>Department of Biology and Biotechnologies “Charles Darwin”, Sapienza University of Rome, Rome, Italy

<sup>e</sup>Department of Biology, University of Padova, Padua, Italy

Corresponding author.

Matteo Cecchetto; [matteocecchetto@gmail.com](mailto:matteocecchetto@gmail.com)

Present address

<sup>f</sup>Department of Environmental Sciences, Informatics and Statistics, Ca' Foscari University of Venice, Venice, Italy

1 **Abstract:**

2

3 One of the main requirements of any sound biological monitoring is the availability of long term and, possibly,  
4 temporal data with a high resolution. This is often difficult to be achieved, especially in Antarctica, due to a variety of  
5 logistic constraints, which make continuous sampling and monitoring activities generally unfeasible. Here we focus on  
6 the 5µm filters used in the desalination plant of the Italian research base "Mario Zucchelli" in the Terra Nova Bay area  
7 (Ross Sea, Antarctica) to evaluate intra-annual coastal nanoplankton dynamics. These filters, together with others of  
8 larger mesh sizes, are used to decrease the amount of organisms and debris in the input seawater before the  
9 desalination processes take place, hence automatically collect the plankton present in the water column around the  
10 desalination system intake. We have used a DNA metabarcoding approach to characterize the communities retained  
11 by filters' sets collected in January 2012 and 2013. Intra-annual dynamics were disclosed with an unprecedented  
12 detail, that would not have been possible by using standard sampling approaches, and highlighted the importance of  
13 extreme, stochastic events such as katabatic wind pulses, which triggered dramatic, short-term shifts in coastal  
14 nanoplankton composition. This method, by combining a cost-effective sampling and molecular techniques, may  
15 represent a viable solution for long-term monitoring programs focusing on Antarctic coastal communities.

16

17 **Keywords:**

18 Antarctica, Ross Sea, Terra Nova Bay, coastal plankton, monitoring, desalination plant, DNA metabarcoding

19

20 **1.1 Introduction:**

21

22 In the last decades, fine-scale studies on plankton diversity have acquired an increasing importance and attention  
23 (Moreira and López García, 2019). Notwithstanding the fact that we are aware that major changes are affecting  
24 oceans' functioning, we still lack an effective and internationally coordinated strategy to better detect the effects of  
25 these changes (Bindoff et al., 2019). The biggest obstacles are due to the intrinsic variability of spatial and temporal  
26 plankton dynamics, coupled with a plethora of methodologies available for plankton biodiversity monitoring. These  
27 two aspects exert a synergistic negative effect, overall causing a limited effectiveness in our capability to draw  
28 meaningful conclusions on ocean ecosystems state and evolution (Navarro et al., 2017; Buttigieg et al., 2018).  
29 Moreover, regardless of the chosen sampling design, biodiversity monitoring programs may be also hampered by

30 logistic constraints, often driven by financial shortcomings, especially when sampling takes place in remote areas  
31 (Lacoursière-Roussel et al., 2018).

32 Traditional methods relying on morphological identification have failed to provide an appropriate solution to these  
33 issues (Gast et al., 2006; Chain et al., 2016; Zhang et al., 2018). These methods, in fact, require a lengthy period of  
34 sample processing time and, in consequence, are generally used on a local-scale, thus leading to higher costs and a  
35 magnification of all the above issues (Baird and Hajibabaei, 2012). They are also affected by low precision and  
36 reproducibility (Baird and Hajibabaei, 2012). One solution proposed to overcome this problem relies on the use of  
37 High Throughput Sequencing (HTS), which gained more attention in the last decade due to its high reproducibility,  
38 short period of processing time and steadily decreasing costs of the analyses (e.g. Taberlet et al., 2012; Valentini et al.,  
39 2016; West et al., 2020).

40 In the Southern Ocean major drivers such as the increase of temperatures, ocean acidification and altered sea ice  
41 dynamics are expected to be the most important factors influencing the future biological communities (Convey and  
42 Peck, 2019). Here, therefore, there is an increasing need of long-term monitoring programs, especially in a  
43 multidisciplinary setting (Convey and Peck, 2019), where fine-scale approaches would be useful to track changes at  
44 high resolution in biological communities.

45 This task, however, is not easy due to the uncomfortable environmental settings typically occurring in polar areas,  
46 where temperatures exceed the freezing point exclusively during the summer months, sea ice conditions may abruptly  
47 change in a short time and sampling activities may be severely hampered by weather conditions. On top of this there  
48 is also the higher cost of maintaining personnel in these remote areas. Thus, operating in Antarctica, the fulfilment of  
49 one of the most important requirements of a sound monitoring program, i.e. a high sampling frequency, it is generally  
50 difficult to be achieved (Proença et al., 2017).

51 This is even more exacerbated in the case of studies of the Antarctic plankton, which is characterized by an intrinsic  
52 extreme dynamism, with composition and vertical carbon export changing in a matter of weeks to days (Bathmann et  
53 al., 1991; Di Tullio et al., 2000; Smith et al., 2003) or even hours, with variations between daytime and night (Celussi et  
54 al., 2009). Moreover, a variety of other local, stochastic factors may further sustain this high dynamism, such as water  
55 column instability driven by strong winds, that may even suppress the development of phytoplanktic blooms (Moline  
56 and Prezelin, 1996) or, in the opposite case, the stratification of the water column in a time frame of days or even  
57 hours due to absence of wind-induced mixing (Brandini, 1993). Also coastal pack-ice dynamics can introduce further  
58 local variability by moving the location of the sea ice marginal zone and hence the seeding of phytoplanktic blooms

59 (Mangoni et al., 2009), with effects varying at the regional spatial scale and at the seasonal time scale (Dayton et al.,  
60 2013). The availability of high resolution time series for Antarctic plankton is thus a crucial point and, at the same  
61 time, one of the most difficult research and monitoring tasks, always requiring a great effort to be achieved.

62 A possible solution or improvement, for achieving high-resolution time series of Antarctic coastal plankton, could be  
63 the analysis of samples automatically collected by research base desalination plants. These facilities were already used  
64 in a number of ecological studies as an auxiliary sampling methodology for the collection of additional planktic  
65 samples, for the investigation of seasonal variations in the phytoplankton, bacteria and picoplankton (Balzano et al.,  
66 2015), for the monitoring of harmful algal blooms in the proximity of desalination plants (Villacorte et al., 2015), or to  
67 collect invertebrate larvae (Heimeier et al., 2010a, 2010b). Desalination plants are employed wherever freshwater  
68 availability is limited and rely on the use of different pre-treatment filters that intercept water-carried particles and  
69 organisms and prevent system clogging, before the final reverse osmosis process (Wolf et al., 2005; Veerapaneni et  
70 al., 2007). Regardless of the possible technical differences existing in different desalination plants, all these systems  
71 employ filters (usually in form of “bags” and “cartridges”) with decreasing mesh sizes, which are replaced whenever  
72 the pressure inside the filter housing increases, i.e. when they start to clog. Since the freshwater is constantly needed  
73 by research base activities, desalination plants operate continuously, drawing seawater throughout the entire  
74 research base opening season, hence representing a potential source of planktic samples constantly collected.

75 As far as we know, the earliest Antarctic studies of desalination filters were authored about ten years ago by Sewell  
76 and Jury (2009, 2011) and were done at the New Zealand’s “Scott Base” (McMurdo Sound, Ross Sea). In these studies,  
77 desalination plant “primary filters” (100 µm mesh size) successfully collected representative samples of zooplankton  
78 (even without damaging the most delicate larval forms) and disclosed the year-round temporal dynamics of the  
79 Antarctic meroplankton (Sewell and Jury 2009, 2011). These studies were also supported by a qualitative comparison  
80 with standard net tows samples collected during the same days in the vicinity of the base, revealing a similar  
81 composition between desalination plant filter samples and a more traditional sampling strategy (Sewell et al., 2006;  
82 Sewell and Jury, 2009). Sewell and Jury (2009) recognized the many advantages observed by the application of this  
83 method, from the opportunity of sampling regardless of weather and sea ice conditions, to the large amount of  
84 seawater filtered by the desalination plant (Sewell and Jury, 2009, 2011). The high filtered-water quantity also enabled  
85 the collection of rare species that could have been overlooked by using standard plankton net sampling (Sewell et al.,  
86 2006; Sewell and Jury, 2009, 2011).

87 Here, we explore the usefulness of samples obtained from the desalination plant filters of a research base (“Mario  
88 Zucchelli” station, Terra Nova Bay, Ross Sea) combined with highly reproducible molecular metabarcoding analysis  
89 (which further reduce sample processing time, increase data precision and expand the study target to smaller ranges  
90 of planktic organisms’ sizes) to disclose possible changes in the composition of nanoplanktic communities.

91 This research represents a proof-of-concept study, where we have specifically: i) looked for a correspondence  
92 between levels of particulate matter in the seawater and the filter replacement rate, ii) explored the composition and  
93 short-term dynamics of the nanoeukaryotic and particle-attached bacterioplankton communities collected by 5 µm  
94 mesh cartridge filters during the Antarctic summer in 2012 and 2013, iii) addressed some of the potential issues on  
95 the sampling and extraction protocol with the final, future aim of achieving a standardized protocol to be applied on a  
96 more general scale.

97

## 98 **1.2 Materials and methods:**

### 99 **1.2.1 Timeframe of the study and of the considered data sets**

100 The first two objectives of this study employed analyses with a different timeframe. In the first case, all the available  
101 satellite data, as well as the logbook data from the electronic logbook of the desalination plant, from October to  
102 February of 2002 to 2019, were included in the analyses, with the only exception of the 24<sup>th</sup> expedition (2008/2009)  
103 for which no logbook data were available. In the second case, sampling of the desalination plant filters was carried out  
104 in January and February of 2012 and 2013 corresponding to a total activity period of the filters examined spanning  
105 from the 25<sup>th</sup> of January to the 4<sup>th</sup> of February of 2012 and from the 8<sup>th</sup> to the 25<sup>th</sup> of January of 2013. Automatic  
106 Weather Station (AWS) hourly data were downloaded from mid-October to the end of February for both 2012 and  
107 2013, but only those corresponding to the same timeframe of the sampled filters activity time were used. Satellite  
108 data, AWS and 5 µm filter activity time (from the desalination plant logbook) for the entire research base opening  
109 season (mid-October to end of February) of the 2011-2012 and 2012-2013 Italian Antarctic Expeditions (XXVII and  
110 XXVIII) are showed in the supplementary material (Fig. S1 and S2).

111

### 112 **1.2.2 Description of the desalination facility**

113 The Italian research base “Mario Zucchelli” station, hereafter “MZS”, is located in Terra Nova Bay (Fig. 1) and provides  
114 facilities and support for 85 people on average (between research and logistic personnel) operating during the Austral  
115 summer from mid-October to the beginning of February. One of the main facilities is the desalination plant (Fig. 2),

116 which is composed of different pre-filtration steps, leading to the main and final filtration operated by ceramic filters  
117 (Fig. 3). Since MZS operates only during the Austral summer, the desalination plant is closed each year at the end of  
118 the expedition (around middle of February) by pumping air in all pipes and valves in order to prevent freezing during  
119 the Antarctic winter. At the beginning of each season (around mid-October), pipes are therefore fully clean, with no  
120 remaining water from the previous season. The entire MZS desalination plant processes 3.5-4 m<sup>3</sup>/h on average. Only  
121 part of this water enters the true desalination pipeline where the filters operate. Given the total volume of the  
122 pipeline from the intake to the filters (0.24 m<sup>3</sup>) it is possible to estimate that this water mass is replaced  
123 approximately 15 times per hour, i.e. once every 4 minutes.

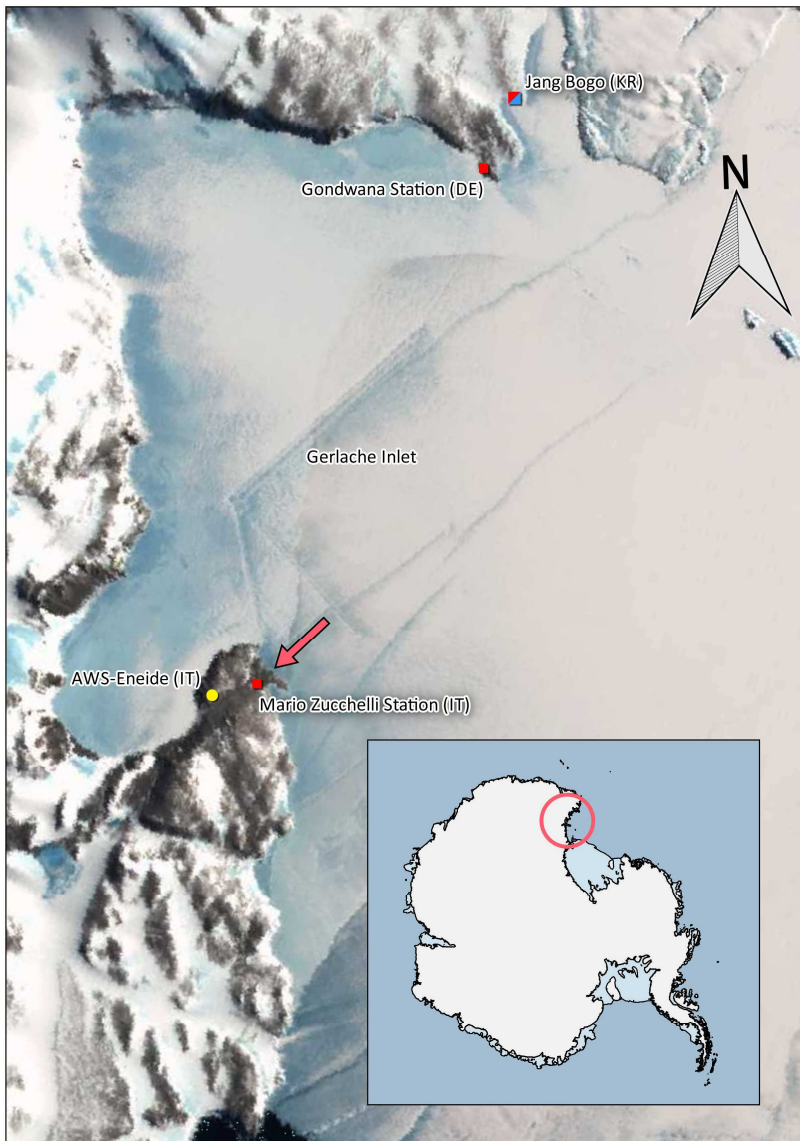


Fig. 1. Overview on Gerlache Inlet (Terra Nova Bay, TNB) showing the three research stations operating in TNB: Mario Zucchelli Station (IT=Italy), Gondwana Station (DE=Germany) and Jang Bogo Station (KR=Republic of Korea). The red squares indicate the research stations operating only during the summer, whereas the red and blue square indicate the only all year-round operating research station (Jang Bogo). The map was produced using the collection of datasets “Quantarctica” (Matsuoka et al., 2018) and the 2.18 version of QGIS (QGIS Development Team, 2020). The map depicts the coastline orientation before the desalination plant seawater intake pipe (red arrow) in the locality of Punta Stocchino and of the Automatic Weather Station (AWS) “Eneide” (yellow circle).

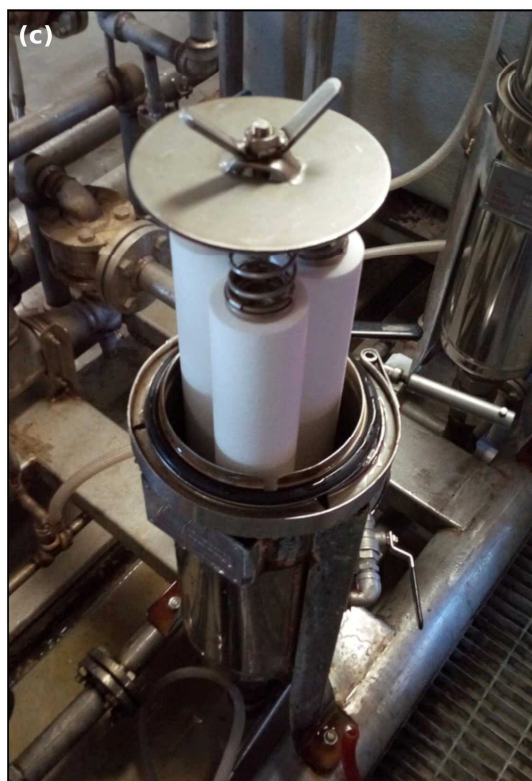
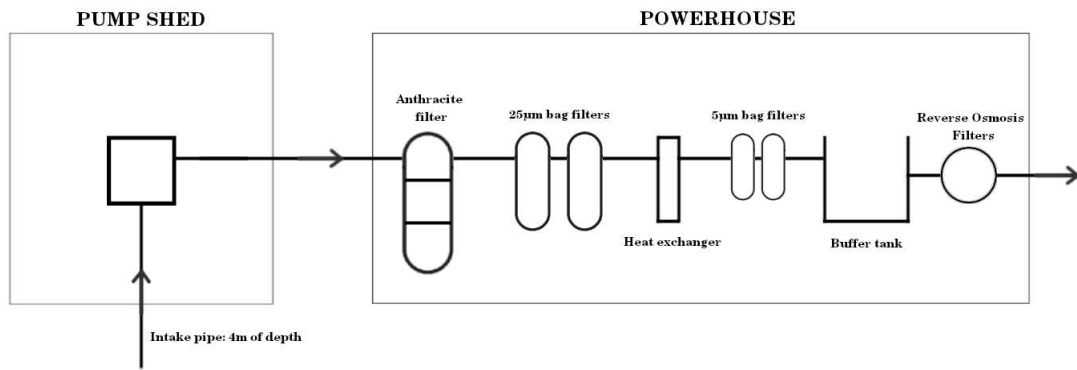


Fig. 2.

Desalination plant of Mario Zucchelli station. (a) View of the plant pump shed in the locality of Punta Stocchino. (b) 25  $\mu\text{m}$  (left) and 5  $\mu\text{m}$  (right) filter housings in the desalination plant powerhouse. (c) New cartridge filters (5  $\mu\text{m}$ ) just replaced before the closure of the lid of the filter housing.



Fig. 3. Simplified diagram of MZS desalination plant.



126

127 The desalination facility starts with the seawater intake pipe (-74.6936°, 164.1185°), opening at a depth of 4 meters in  
128 the locality of "Punta Stocchino". From there, a series of pipes (diameter of 2 inches) and valves allow the water to  
129 flow directly to the main powerhouse, distant approximately 120 meters from the intake pump shed. Here the first  
130 steps of filtration are obtained through a filter packed with anthracite, followed by polyester bag filters of 25 µm mesh  
131 size, a heat exchanger (which brings the seawater temperature to 10° C to maximize the efficiency of the final ceramic

132 filters) and a final set of filters made by polypropylene cartridges of 5  $\mu\text{m}$  mesh size, which were the focus of the  
133 present analysis.

134 The electronic logbook of the desalination plant was inspected to gather all the available historical records for  
135 cartridge and bag filters activity and replacement, as well as the amount of consumed water at the research base. All  
136 the timings for the filter replacements, together with the activation and turn-off of the desalination plant for technical  
137 purposes, are recorded in the logbook. Thus, it is possible to obtain the exact number of hours each filter has been  
138 filtering before its replacement, done in order to avoid reaching the clogging limit.

139 Differently from Sewell and Jury (2009), where 100  $\mu\text{m}$  filters are “reusable” and regenerated after having been in use  
140 the same amount of time, at MZS Station, the 25  $\mu\text{m}$  bag and 5  $\mu\text{m}$  cartridge filters are disposable, hence discarded  
141 after use. Their smaller mesh size, in fact, makes any potential regeneration process unsuitable. Collected plankton  
142 samples for analyses are thus not obtained by washing the filters as in Sewell and Jury (2009), but only by the  
143 disruption of the filter structure (see below). In our case each filter is changed when the pressure inside the cartridge  
144 filter housing reached high levels, meaning that similar levels of plankton biomass and particulate matter are  
145 collected, regardless the amount of filtered seawater or time of activity, although this datum is always recorded in the  
146 logbook.

147

### 148 **1.2.3 Sampling and laboratory procedures**

149 Sampling was carried out in January and February of 2012 and 2013 enabling the collection of a total of eleven 5  $\mu\text{m}$   
150 cartridge filters, five in 2012 and six in 2013. The starting day for the two time ranges refers to the day in which the  
151 first filter was installed, differently from the sample name, which identifies the day it was sampled. For example, the  
152 filter “30\_1\_12” sampled the 30<sup>th</sup> of January of 2012 was installed 115 hours earlier, thus the 25<sup>th</sup> of January is the  
153 starting day for the time range investigated during 2012. The volume of water treated by the filters, based on data  
154 from the desalination plant electronic logbook, ranged from a minimum of 12.7 to a maximum of 64.8  $\text{m}^3$ , with an  
155 average of approximately 23.41  $\text{m}^3$  per filter. The sea was in ice-free conditions from at least ten days before our  
156 sampling (Illuminati et al., 2017; Monti et al., 2017 for 2012; Schiaparelli personal communication for 2013). As soon  
157 as the pressure inside the cartridge filter housing reached high levels, the desalination plant technician informed one  
158 of the authors (SS) of the imminent replacement and let all the remaining seawater in the housing to flow  
159 “downstream” to the next desalination step. At this point filters were removed from the housing using lab gloves,  
160 placed in a sterile plastic bag and then stored at  $-20^\circ\text{C}$ . These filters (Fig. 4a), measuring 50.8 cm of length and 6.4 cm

161 of diameter, were kept at -20° C until summer 2018, when they were processed for the molecular analyses. Three  
162 replicates were obtained from each filter (one at the top, one in the middle and one at the end of the filter in order to  
163 cover all its length, see Fig. 4a), for a total of 33 replicates.



Fig. 4. (a) A frozen cartridge filter sampled on February 4<sup>th</sup> after having filtered ~22.5 hours. The three replicates were sampled from both extremities and the centre (blue arrows). (b) Layers of polypropylene extracted using a cork borer and a pair of heat-sterilized tweezers prior to the DNA extraction. Successively, the layers were cut in half and then in stripes of 1 mm of width.

164

165 A metal, cylindrical, autoclave-sterilized cork borer of 26.25 mm in diameter was used to carve a circular cut on the  
166 surface of the cartridge filter. Different subsampling protocols were attempted on unused filters weeks before  
167 processing the filters used for this study, and tested by evaluating the amount and quality of the extracted DNA.  
168 During this optimization of the subsampling protocol, the deepest layers were found to yield a low amount of DNA.  
169 The most exterior layer of the filter (< 1 mm) was peeled off using a pair of heat-sterilized tweezers, in order to avoid  
170 any potential risk of post-sampling contamination, and discarded. Molecular analyses were thus performed on the  
171 immediately lower layer of the filter, and multiple cuts were performed for each replicate on different sides of the  
172 filter, enabling the extraction of the appropriate amount of sample weight required by most DNA extraction kits (i.e.  
173 at least the 0.3 g for the DNeasy PowerSoil Kit), also optimizing the amount of recoverable DNA.

174

#### 175 **1.2.4 Molecular analyses**

176 Filter layers from each replicate were cut into small stripes (<1 mm) and then placed in the PowerBead Tubes  
177 provided by the DNeasy PowerSoil Kit (QIAGEN). DNA was extracted following the manufacturer's instructions, with  
178 the exception of an additional incubation step with the C1 solution in a thermostatically controlled water bath (70° C  
179 for 10 minutes) and a final elution with 50 µl (instead of 100) of the C6 solution, in order to increase the DNA  
180 concentration. PCR amplification and sequencing of fragments of the 16S rRNA and 18S rRNA genes, for bacteria and

181 eukaryotes respectively, were performed by IGA Technology (Udine, Italy, <https://igatechnology.com/>). The primers  
182 used for the V3 and V4 regions of 16S rRNA gene (approximately 450 bp) were chosen from Herlemann et al. (2011)  
183 and have the following sequences (Illumina adapters underlined): 341F - 5'  
184 TCGTCGGCAGCGTCAGATGTGTATAAGAGACAGCCTACGGGNGGCWGCAG 3' and 805R - 5'  
185 GTCTCGTGGGCTCGGAGATGTGTATAAGAGACAGGACTACHVGGGTATCTAATCC 3'. The primers used for the V4 and V5  
186 regions of the 18S rRNA gene (approximately 550 bp) were selected from Hugerth et al. (2014) and have the following  
187 sequences (Illumina adapters underlined): 574\*F - 5'  
188 TCGTCGGCAGCGTCAGATGTGTATAAGAGACAGCGGTAAYTCCAGCTCYV 3' and 1132R - 5'  
189 GTCTCGTGGGCTCGGAGATGTGTATAAGAGACAGCCGTCAATTHCTTYAART 3'. The PCR mix was the same for both  
190 markers and consisted in 12.5 µl of 2x KAPA HiFi HotStart ReadyMix (Kapa Biosystems, Woburn MA, USA), 5 µl of each  
191 primer and 2.5 µl of microbial DNA at a concentration of 5 ng/µl. The amplification conditions were: 95° C for 3  
192 minutes, 25 cycles of 95° C for 30 seconds, 55° C for 30 seconds and 72° C for 30 seconds, followed by a final step at  
193 72° C for 5 minutes.

194 A PCR clean-up step was performed using AMPure XP beads (Beckman Coulter) to purify from free primers and primer  
195 dimer species. This was followed by an indexing step using the Nextera XT Index (Illumina), to attach dual indices and  
196 Illumina sequencing adapters. The PCR program was the same of the amplicon PCR, except for the number of cycles  
197 set to 8 instead of 25. Another PCR clean-up step was performed prior to the quantification, normalization and  
198 sequencing using Illumina MiSeq v3 reagents on a 300 bp paired end reads MiSeq platform.

199 The PCR amplicons of the 16S rRNA region were sequenced on two different MiSeq runs to reach the minimum  
200 number of agreed sequences, which was 200,000 paired-end reads per replicate. All fastq files generated in this study  
201 are available in Mendeley Data (<http://dx.doi.org/10.17632/89xmbhsgvc.1>).

202

### 203 **1.2.5 Bioinformatic analyses**

204 Raw 18S rRNA sequences, after demultiplexing, were quality checked using FastQC and paired-end reads were merged  
205 using Vsearch (Rognes et al., 2016), excluding merged products with more than 1 ambiguous base and more than 3  
206 differences in the alignment. Primers were removed using Cutadapt (Martin, 2011), allowing only one error in the  
207 alignment. Mothur (Schloss et al., 2009) was adopted to remove sequences with homopolymers greater than 8 bases,  
208 whereas Vsearch was used to remove all sequences with a maximum expected error of 1, for length filtering (max 580  
209 bp and min 490 bp) and for the dereplication. After the dereplication, the UNOISE2 algorithm (Edgar, 2016)

210 implemented within USEARCH (Edgar, 2010), using the command “unoise3”, was used to check for chimeras and  
211 remove singletons, generating the Zero-radius Operational Taxonomic Units (ZOTUs) fasta file. Vsearch was used again  
212 for the creation of a count table (command “usearch\_global”) using a global pairwise alignment with id equal to 1. The  
213 taxonomic assignment was conducted using the “Wang method” (naïve Bayesian classifier; Wang et al., 2007)  
214 implemented in Mothur and using version 4.12.0 of the PR<sup>2</sup> database (Guillou et al., 2013).

215 Raw 16S rRNA sequences were processed with the same programs as for 18S rRNA, but with the following differences:  
216 the maximum differences allowed for merging were set to 10 (due to the longer alignment region for that primers),  
217 concatenation of the fastq files of the two different runs for each replicate, maximum expected error set to 0.5, length  
218 filtering set to 430 and 400 of maximum and minimum length respectively and the original (i.e. not modified) mothur-  
219 formatted version of the Silva database (release 132) for the taxonomic assignment (Quast et al., 2012).

220 The following bioinformatics analyses were all undertaken in R (version 3.6.3, R Core Team, 2020) and Qiime2 (Bolyen  
221 et al., 2019). A variance stabilizing transformation, implemented in the R package DESeq2 (Love et al., 2014) was  
222 applied to account for differences in the number of sequences, without prior merging of all the replicates. This  
223 stabilization was introduced as an alternative to the more common rarefaction method (McMurdie and Holmes,  
224 2014). Negative values, which in the context of a variance stabilizing transformation indicate that in the original count  
225 table those values were more likely to be zero, or in any case negligible, were approximated to 0, as suggested by the  
226 phyloseq authors (McMurdie and Holmes, 2013)  
227 (<https://www.bioconductor.org/packages/release/bioc/vignettes/phyloseq/inst/doc/phyloseq-FAQ.html#negative->  
228 [numbers-in-my-transformed-data-table](https://www.bioconductor.org/packages/release/bioc/vignettes/phyloseq/inst/doc/phyloseq-FAQ.html#negative-numbers-in-my-transformed-data-table), last access on October 07 2020). This approximation allowed the calculation  
229 of Bray-Curtis distances for the ordination plot generated through a Non-metric Multidimensional Scaling (NMDS)  
230 using phyloseq. The Mantel test for evaluating a correlation between the distance matrices of 18S rRNA and 16S rRNA  
231 datasets was performed using qiime2. Heatmaps were produced using the phyloseq R package, following the  
232 phyloseq-specific implementation of the NeatMap approach (Rajaram and Oono, 2010), adopting an ordination  
233 method instead of a hierarchical cluster analysis. Both heatmaps were calculated on Bray-Curtis distances and with a  
234 NMDS ordination. The heatmap for the 18S rRNA dataset was produced after reducing the count table to the 50<sup>th</sup>  
235 most abundant ZOTUs sorting samples by chronological order, from the 30<sup>th</sup> of January to the 5<sup>th</sup> of February of 2012  
236 and from the 11<sup>th</sup> to the 25<sup>th</sup> of January of 2013. The heatmap for the 16S rRNA dataset was produced after reducing  
237 the count table to the 1000<sup>th</sup> most abundant ZOTUs, agglomerating them at the order level (fourth taxonomic level of

238 the Silva Database) and sorting samples by chronological order. Taxa barplots were generated using phyloseq from the  
239 original, not transformed, count table after collapsing together all the replicates in the respective samples.

240

#### 241 **1.2.6 Environmental data: air temperature, wind and chlorophyll**

242 AWS data on surface air temperature and wind direction and velocity were obtained from the “MeteoClimatological  
243 Observatory at MZS and Victoria Land” of PNRA ([www.climantartide.it](http://www.climantartide.it)), for the AWS “Eneide” (-74.6959°, 164.0921°),  
244 located approximately 820 meters from the desalination plant pump shed. Data were processed in R using the  
245 packages “oce” (Kelley and Richards, 2019), “signal” (signal developers, 2013), “tsibble” (Wang et al., 2019), “dplyr”  
246 (Wickham et al., 2019) and “cowplot” (Wilke 2019).

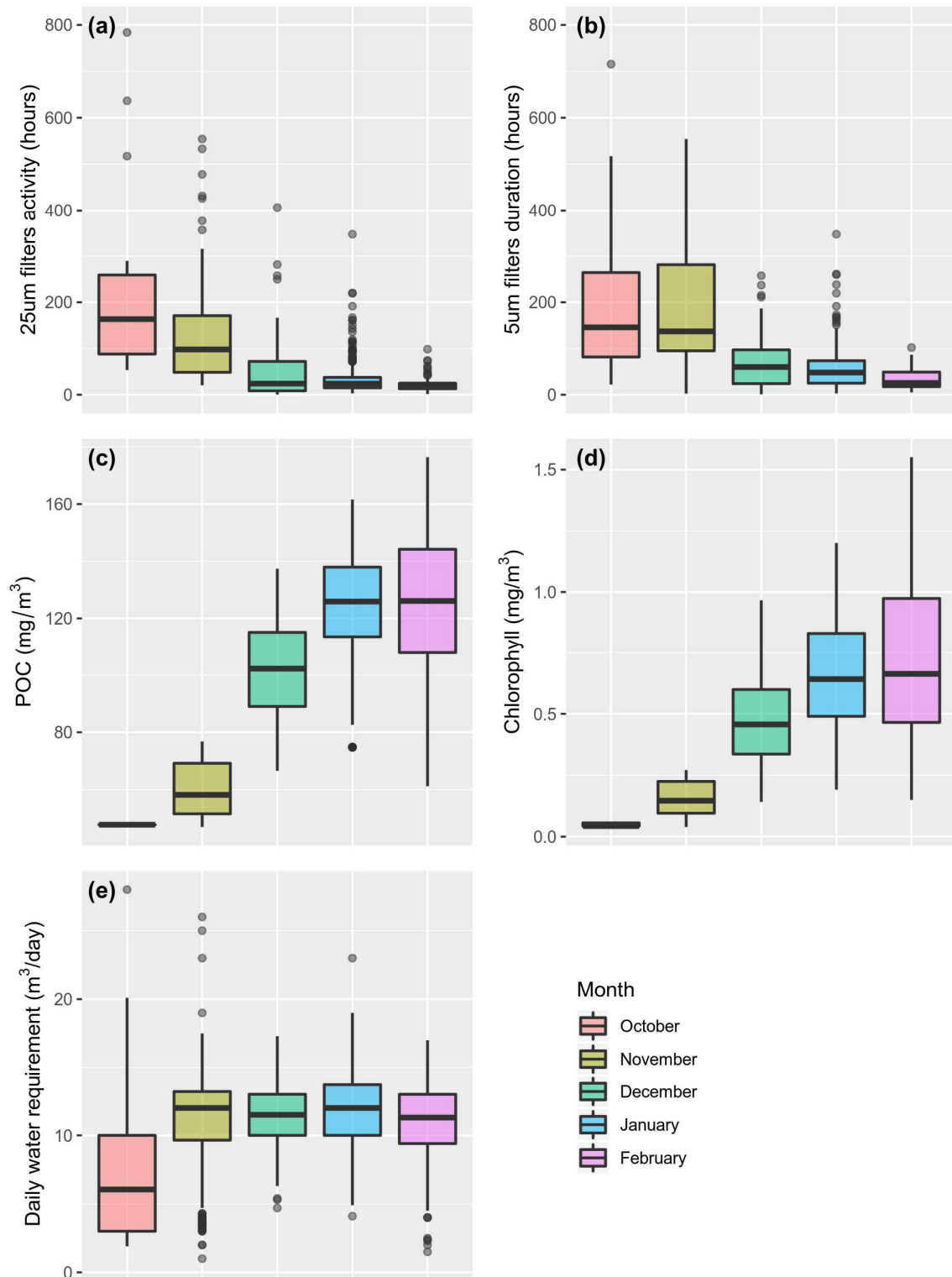
247 Satellite data on chlorophyll (Ocean Biology Processing Group 2018a) and POC (Ocean Biology Processing Group  
248 2018b) concentrations were obtained from NASA's OceanColor Web site using the level-3 browser to extract daily and  
249 monthly climatology data (from October to February of each year). Data were extracted choosing the “Standard”  
250 product at a 4 km resolution grid and for the area with the following latitudinal and longitudinal bounding box: -74.5°,  
251 -75°; 163.5°, 165°. The downloaded mapped files were converted from the format NetCDF to “csv” (comma separated  
252 values) using GDAL (Geospatial Data Abstraction Library, GDAL/OGR contributors 2020) and processed in R using the  
253 “ggplot2” package (Wickham 2016).

254 **1.3 Results and Discussion**

255 **1.3.1 Particulate matter and filter replacement rate**

256 Logbook data on filtering activity for filter cartridges (5  $\mu\text{m}$ ) and bags (25  $\mu\text{m}$ ) from 2002 to 2019 showed a consistent  
257 decrease in filtering activity hours from October to February, resulting in a higher rate of filter replacement towards  
258 the end of the summer (Fig. 5a and b). This observed higher rate of filter replacement since the end of the summer  
259 could be due to two different reasons: i) an increase of the desalination plant activity because of the intensification of  
260 the logistic activities in the research station, or ii) a progressive increase of the particulate matter present in the  
261 seawater. However, it is clear that the decreased filtering time in summer is not due to the logistic and scientific  
262 activities as the daily water requirement shows no particular trend (Fig. 5e) while, on the contrary, there is a clear  
263 increase of chlorophyll and POC from October to February (Fig. 5c and d). A more detailed overview on the temporal  
264 dynamics of filter replacement rate, with hourly and daily recordings of environmental variables throughout the 2011-  
265 2012 and 2012-2013 opening seasons, is provided in the supplementary material (Fig. S1 and S2).

Fig. 5. Boxplots of log-diary and satellite data from 2002 to 2019. Upper boxplots refer to (a) filter activity hours for bag filters (25  $\mu\text{m}$  mesh size) and (b) cartridge filters (5  $\mu\text{m}$  mesh size). Boxplots in the middle refer to (c) Particulate Organic Carbon (POC) and (d) Chlorophyll concentration measured in milligrams per cubic meter. Lower boxplot (e) refers to the total monthly cubic meters of water consumed by the research station. All data has been gathered based on month of registration and ordered from October to February. Satellite data for Chlorophyll and POC in October are less abundant than for the other months, as most of the area is usually covered in sea-ice during that period. Filters were assigned to month on the base of their installation time.





267 This means that when the phytoplanktic bloom takes place, the increased amount of biomass in the seawater  
268 progressively and comparably determine an increase in the filter replacement rate, with a dramatic transition from  
269 weeks of activity of a single filter to peaks of multiple changes of filters per day. This situation takes place every year  
270 during Antarctic summer, in conjunction with the sea ice retreat and the occurrence of phytoplanktic blooms triggered  
271 by sympagic communities (Mangoni et al., 2009; Saggiomo et al., 2017). The distribution of blooms is rather patchy,  
272 being influenced by the seasonal extension and shape of the marginal ice-zone. This determines a mosaic of different  
273 planktic communities in the water column, each one characterized by a different taxonomic composition (Nuccio et  
274 al., 2000). Other environmental drivers, such as winds, may introduce other sources of variability, further affecting  
275 community dynamics (Brandini, 1993; Moline and Prézelin, 1996; Fitch and Moore, 2006). The effect of wind is  
276 especially important in Antarctica due to the existence of high-energy winds, i.e. katabatic winds, whose pulses can be  
277 considered extreme events.

278 Thus, due to the high community patchiness and the presence of major environmental drivers, the availability of a  
279 higher sampling frequency is mandatory in order to unravel intra and inter-annual planktic dynamics, especially when  
280 it is know that rapid short-term variations have a high probability of occurrence as also shown by our data.

281

### 282 **1.3.2 Community composition, diversity and dynamics of nanoplankton revealed by DNA metabarcoding**

283 Bioinformatics analyses produced a total of 603 ZOTUs for 18S rRNA and 3,914 ZOTUs for 16S rRNA. Final abundance  
284 values add up to 1,219,853 and 1,726,680 sequences, corresponding to ~30% and ~38% of the total “raw” sequences  
285 for the 18S rRNA and 16S rRNA datasets, respectively.

286 The NMDS (Fig. 6) showed the ability of amplicon sequencing to differentiate nanoplanktic communities investigated  
287 during similar seasons of two consecutive years and to track short-term changes in community composition taking  
288 place just in a few days (Fig. 6). For both years the ordination showed a clear distinction between the first days and  
289 the following ones, meaning that the investigated time frame was characterized by a transition of the community  
290 composition from a particular state to another one. The same transition has been recorded both in the 16S rRNA and  
291 18S rRNA datasets (Fig. 6), suggesting that the different environmental and biological conditions similarly influenced  
292 both communities, with a very neat and strict positive correlation between the two Bray-Curtis distance matrices  
293 (Pearson  $r=0.90387$ ,  $p=0.001$ ) (Fig. 7). Thus, any change in community composition can be tracked by DNA  
294 metabarcoding using alternatively 16S rRNA or 18S rRNA, which provide highly overlapping metrics.

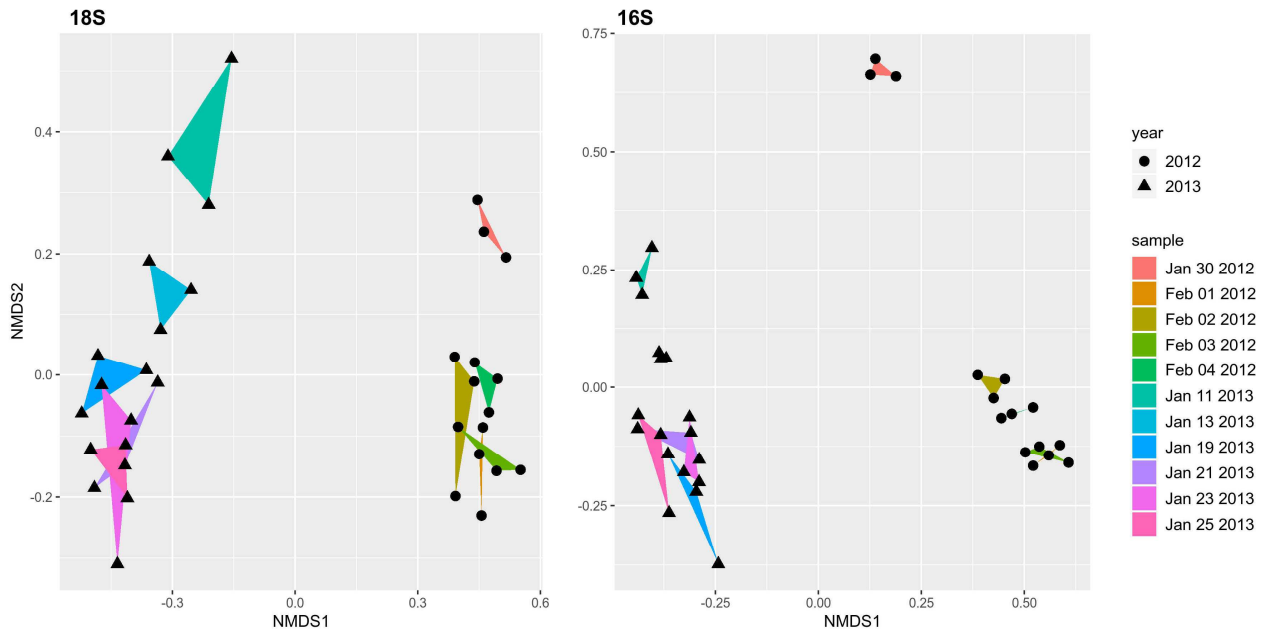


Fig. 6. Non-metric Multidimensional Scaling of 16S and 18S based on Bray-Curtis distances. Colours refer to the replicates of the same filter, thus corresponding to the same day of sampling. Dates in the legend are ordered in temporal succession. Triangles refer to 2012 samples and circles to 2013 samples.

295

296

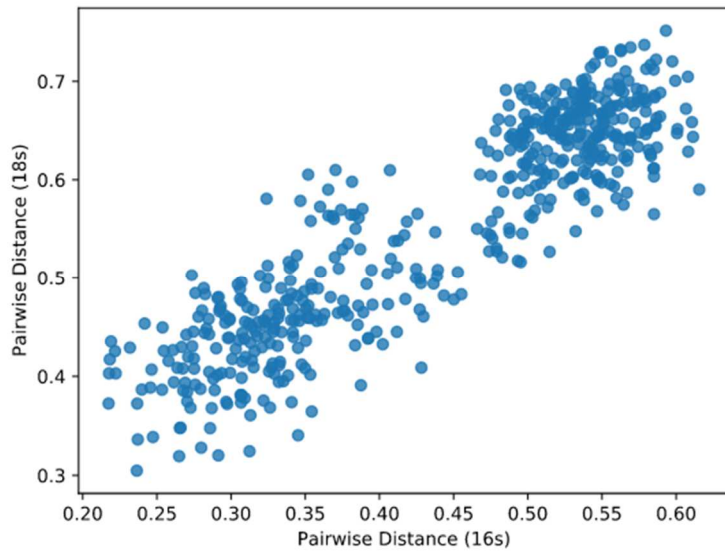


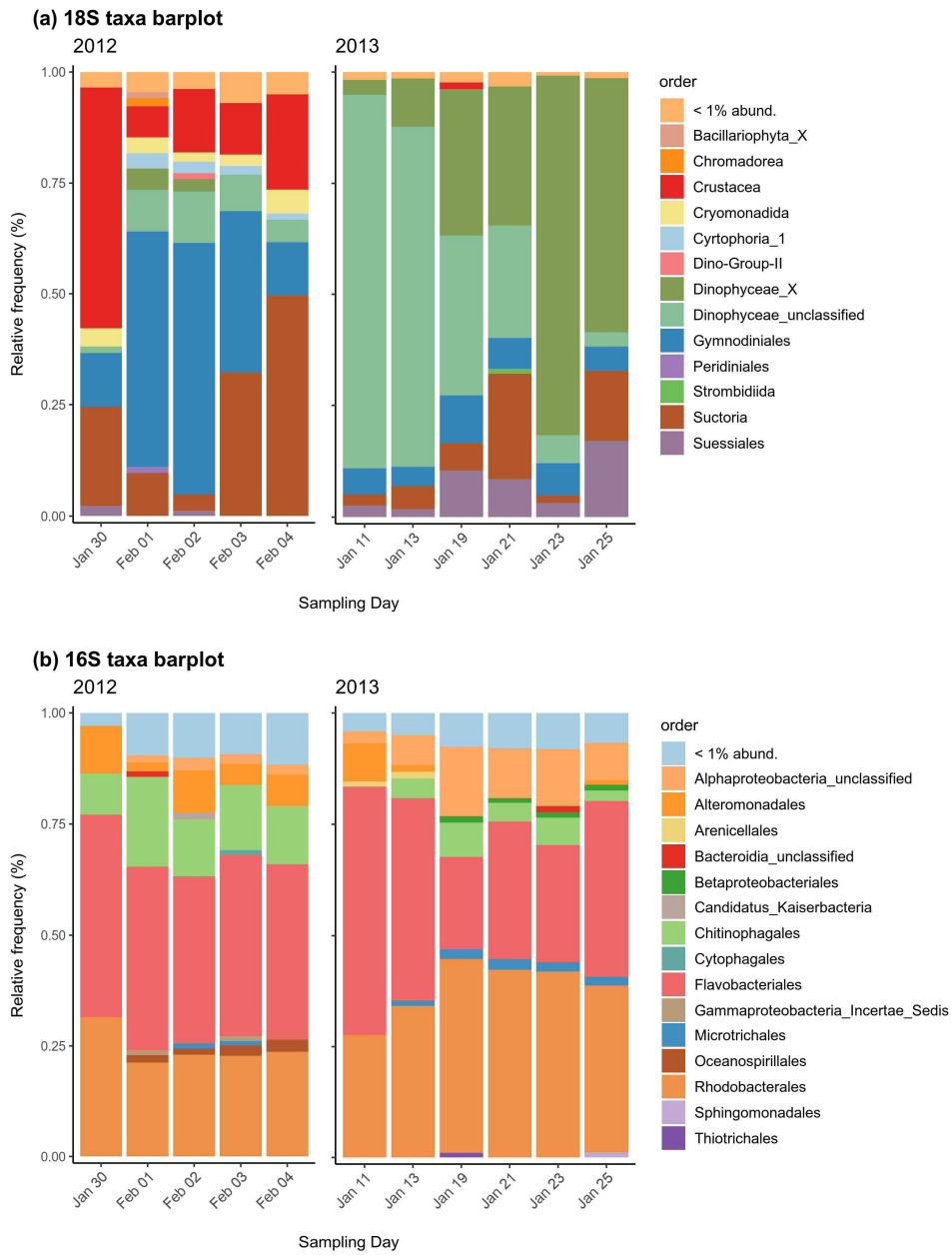
Fig. 7. Scatterplot showing the correlation

between the two different matrices of Bray-Curtis distances for 18S and 16S.

297

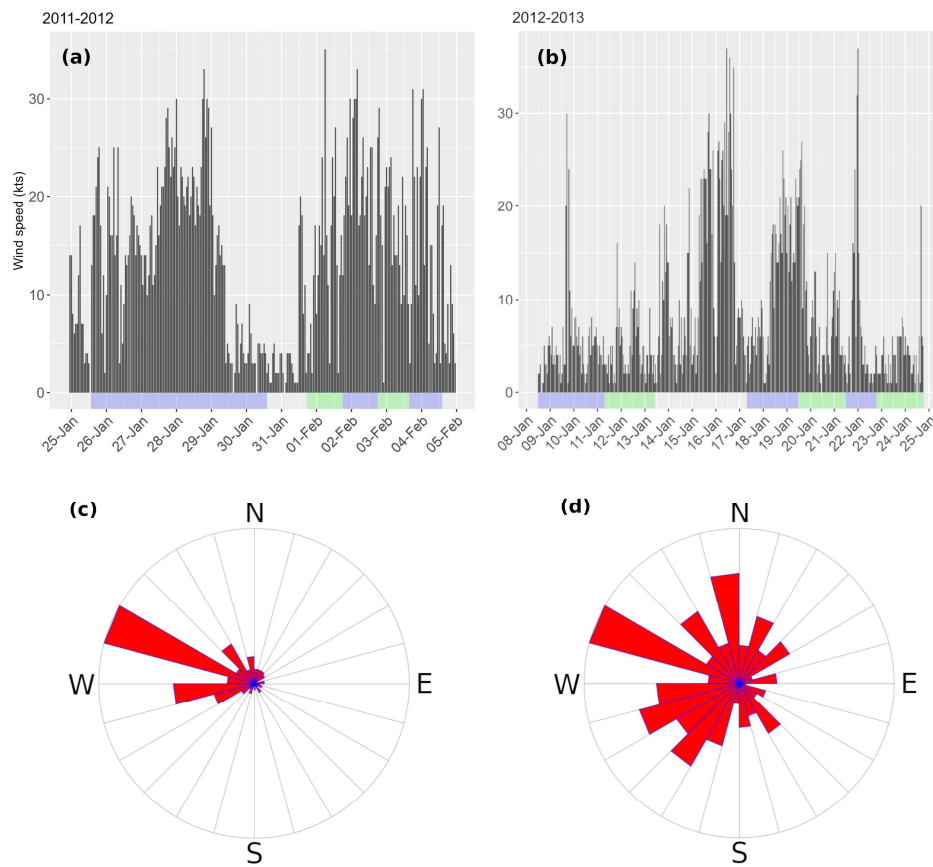
298 The nanoeukaryotic community here investigated showed a marked presence of different taxonomic groups of  
 299 Dinophyceae in both years. The 2012 dataset was characterized by the presence of Gymnodiniales and a more  
 300 relevant incidence of Metazoa (Arthropoda, Maxillopoda) and Suctoria (Ciliophora, Phyllopharyngea), while in January  
 301 2013 two unidentified groups of Dinophyceae resulted to be the most abundant taxa (Fig. 8a). The 16S rRNA dataset  
 302 showed a community resembling the typical composition of surface waters Antarctic copiotrophic prokaryotes, being  
 303 dominated by the classes Bacteroidia, Alphaproteobacteria and Gammaproteobacteria, already evidenced in previous  
 304 studies (Celussi et al., 2010; Lo Giudice et al., 2012; Lo Giudice and Azzaro, 2019) (Fig. 8b). However, due to the mesh  
 305 size of the cartridge filters, the bacterioplankton community here investigated should not be referred to free-living  
 306 bacteria, but rather to particle-attached prokaryotes.

Fig. 8. (a) Taxa barplots for 18S of 2012 (left) and 2013 (right). (b) Taxa barplots for 16S of 2012 (left) and 2013 (right).



308 The two different time ranges investigated also indicate different intra-annual dynamics: in 2012 there was a  
309 temporary (lasting only three days, from the 1<sup>th</sup> to the 3<sup>th</sup> of February) increase of the relative frequency of  
310 Gymnodiniales and other orders of Dinophyceae over Maxillopoda and Suctoria, while in 2013 there was a clear shift  
311 between two distinct groups of Dinoflagellates, represented in particular by the class Dinophyceae (Fig. 8a).  
312 The abrupt change in the community composition detected in 2012 may be the result of a water column instability  
313 induced by katabatic wind pulses that, as shown by the AWS "Eneide" data (Fig. 9a and c), characterized two distinct  
314 periods of high wind intensity separated by an interval of 3 days with low-intensity winds (January 29<sup>th</sup> - February 1<sup>th</sup>).  
315 During this brief period of calm weather and water column stability there was an increase of different groups of  
316 Dinoflagellates, but this did not lead to a monospecific bloom, which was likely disrupted by the second katabatic  
317 event.

Fig. 9. Barplots of hourly wind speed recordings (a,b) and wind roses (c,d) for the two different time ranges investigated during 2012 and 2013. (a) The wind intensity (knots) and (c) wind rose at the bottom for the 2012 series, (b) and (d) for the 2013 series. Blue and green bands below the barplots indicate activity time ranges for the individual filters sampled for this study, whereas the grey areas represent the activity time of filters that couldn't be sampled for this study.



318

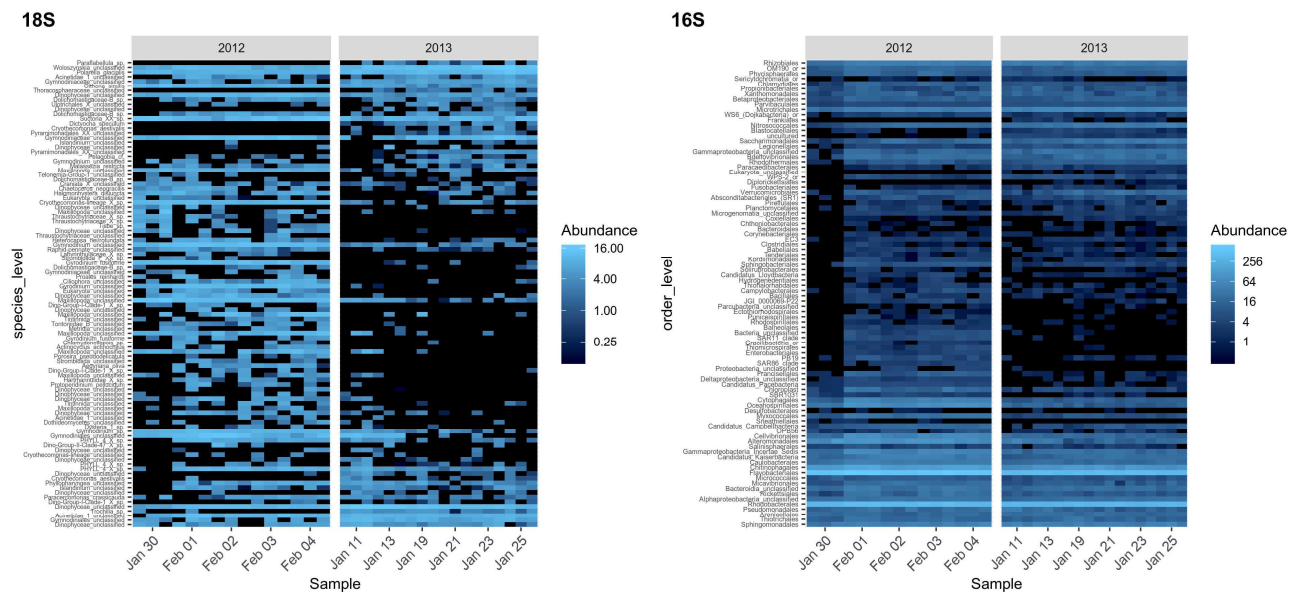
319 The high presence of Maxillopoda sequences registered during periods of high wind intensity should not be  
 320 considered as indicative of the presence of crustacean adults on the cartridge filter itself, but as a possible result of  
 321 spawning or molting events or even from disrupted body parts originating from individuals intercepted from upstream  
 322 components of the desalination plant. The latter would be more likely, especially if we consider the equally high  
 323 presence of Suctorian sequences, which are the most widespread symbiotic group in the phylum Ciliophora and can  
 324 be found as facultative ectosymbionts on crustaceans (Lynn, 2008) or even on phytoplankton (Sazhin et al., 2007).

325 On the other hand, no katabatic event was recorded by the AWS during the 2013 time series, resulting in a relatively  
326 calm period with just sporadic peaks of wind intensity from different directions (Fig. 9b and d). These more stable  
327 conditions may have favoured a progressive shift between two different Dinoflagellate groups, without abrupt  
328 changes as those observed in the 2012 series.

329 Regarding the bacterioplankton community, the distinction in the community composition (Fig. 6) is likely to be  
330 determined by an increase in the relative abundance of Rhodobacterales (Alphaproteobacteria) and an unidentified  
331 group of Alphaproteobacteria, mostly to the detriment of Gammaproteobacteria and of Flavobacterales (Bacteroidia).

332 For the 2012 series, no evident temporal dynamics at higher taxonomic levels can be appreciated and the major  
333 difference inferred by the NMDS is likely to be the result of an abrupt increase in alpha diversity between the first day  
334 (January 30<sup>th</sup>) and the following ones (Fig. 10). The orders Chitinophagales (Bacteroidia) and Alteromonadales  
335 (Alphaproteobacteria) were the only ones showing a slight increase and decrease (Fig. 8b) in percentage, respectively,  
336 probably reflecting the increase in phytoplanktic activity and algal-derived polymeric substrates (Wilkins et al., 2013)  
337 of both dinoflagellates and diatoms.

Fig. 10. Heatmap of 18S 50 most abundant ZOTUs (left) and 16S 1,000 most abundant ZOTUs (right), the latter agglomerated by taxonomic order (fourth level from the highest of the Silva database taxonomy). Abundances values refer to those given after the variance stabilizing transformation. The x-axis is sorted in chronological order, from the oldest to the most recent filter, with the 2012 series on the left and the 2013 on the right, for both heatmaps.



338

339 The correlation between low wind activity and the development of phytoplanktic blooms has already been  
 340 recognized, not only in Antarctic coastal planktic communities (e.g. Brandini, 1993, Moline and Prezelin, 1996), but  
 341 also in Antarctic offshore areas (e.g. Sallée et al., 2015; Kanta et al., 2017; Park et al., 2019), as well as in non polar  
 342 areas (e.g. Nieblas et al., 2009; Qu et al., 2020). High wind activity has a direct effect on the water column structure,  
 343 being capable of mixing it and inducing upwelling phenomena, thus hampering bloom occurrences (Tripathy and Jena,  
 344 2019).

345 Our data showed a sudden temporal response of these communities after the reduction in wind intensity, which may  
 346 have allowed a temporary condition of stability that, in turn, enabled the start of a water column stratification  
 347 process. This was reflected in the increase in dinoflagellate abundance, which, however, couldn't last more than three  
 348 days due to the occurrence of a second katabatic event.

349 Unfortunately, most of the research based on HTS methodologies conducted in Terra Nova Bay (and especially near  
 350 the Italian Research station "MZS") focused on prokaryotic communities only (Lo Giudice and Azzaro, 2019) and not  
 351 on the eukaryotic ones. Consequently, the absence of an in depth knowledge of coastal eukaryotic communities  
 352 studied through metabarcoding hampers a critical comparison with our results. Nonetheless, the data obtained in this  
 353 study showed a clear dominance of dinoflagellates in the nanoplanktic community, in accordance to what is known  
 354 from previous study focusing on deeper water strata (Zoccarato et al., 2016) or on the sea ice (Torstensson et al.,



355 2015), suggesting that these groups may play a very important and general role in Antarctic ecosystems (Liu et al.,  
356 2020). The absence of other protists, such as Radiolaria, Hacrobia and Excavata (which, apart from the latter, are  
357 nonetheless represented by some ZOTUs in the dataset), may be due to the difference in the size range investigated,  
358 wider in the aforementioned studies or simply to the intrinsic differences in the water masses examined or in the  
359 timing of sampling.

360 Several highly represented taxa in our results have never or only just rarely been documented in this area before. This  
361 is the case of some groups of eukaryotes such as: i) Cryomonadida (Cercozoa; Filosa-Thecofilosea), which graze on  
362 bacteria and may also parasitize phytoplankton (Zoccarato et al., 2016); ii) Cyrtophoria (Ciliophora; Phyllopharyngea),  
363 typically found in biofilms or as facultative or obligate symbionts on the body surfaces of invertebrates, such as  
364 crustaceans (Lynn, 2008); and iii) Suctorina (Ciliophora; Phyllopharyngea), this latter one representing the third most  
365 abundant taxon in the entire 18S rRNA dataset. The absence of diatoms in high number is a more surprising result,  
366 and will be discussed later in the next section.

367 However, regarding the comparison of inter-annual dynamics, it has to be stressed that no conclusions can be drawn  
368 despite the sampling activities occurred in the same season and with a similar timing. In fact, the investigated time  
369 ranges are too short and it is not possible to assess whether or not the two observed situations represent “typical”  
370 seasonal dynamics, just shifted in time. A more comprehensive analysis, embracing the whole Austral spring and  
371 summer months of the Antarctic field season 2018-2019 is currently under study (Cecchetto et al. unpublished results)  
372 and will be of help in understanding these dynamics.

373

### 374 **1.3.3 Advantage of the method and possible implementations**

375 Despite only few filters were available for this study, also limited only to the 5 µm mesh size fraction, our molecular  
376 approach enabled a high-resolution analysis of intra-annual dynamics of Terra Nova Bay plankton. This was obtained  
377 through a cost-effective method (no funds were needed to set up the filtering system as it is part of the research base)  
378 and, especially, without the need of personnel at sea for continuous samplings, which is logistically unfeasible  
379 especially during extreme weather conditions that characterize katabatic wind events. Several new taxa were also  
380 recorded for the first time and future studies will enable clarifying if these are regular occurrences in the area.

381 Unfortunately, not enough filters have been studied so far in order to address the capacity of recovering rare taxa  
382 based on the different amount of filtered seawater, as most of the filters were in use for a similar amount of hours  
383 (see materials and methods). Sewell and Jury (2009) stated that the system is capable of recovering most of the rare

384 taxa, but their methodology allowed a sampling frequency based on the quantity of seawater filtered, whereas in our  
385 study this approach would be logistically unfeasible. Only a couple of filters (the first of the two series) had  
386 significantly higher values of filtered seawater but, as mentioned earlier, they also were those with the lower numbers  
387 of taxa recorded.

388 Moreover, as the amount of particulate present in the input seawater does not necessarily correspond to higher  
389 biomass, uncertainties in the interpretation of actual bloom events may arise. This issue could be easily resolved by  
390 monitoring also other environmental and biological parameters (e.g. turbidity and chlorophyll concentration) by  
391 establishing an *in situ* monitoring station located in the vicinity of the seawater intake pipe to obtain environmental  
392 data *in continuum*. The availability of these data will enable a more precise interpretation of the community changes  
393 disclosed by metabarcoding.

394 It has also to be considered that in metabarcoding studies the abundances of taxa are always difficult to be estimated  
395 in “absolute” terms for a variety of reasons (Taberlet et al., 2018), above all the well-known issues regarding primer  
396 amplification biases (Jovel et al., 2016; Piñol et al., 2018). The adoption of different methodologies, such as  
397 metagenomics (adopting shotgun sequencing techniques), which don’t rely on amplification enrichment, would  
398 certainly reduce the impact of these issues (Bohmann et al., 2014). In this context, biodiversity monitoring using filters  
399 from desalination plants, and its usefulness in detecting short-term dynamics in coastal communities, would greatly  
400 benefit from the potentials of methodologies such as metatranscriptomics. In general, further and specific research  
401 would be required to validate the applicability of different methodologies, also according to the taxonomic group of  
402 interest, the project goals, and the availability of *in situ* lab facilities.

403 Some eukaryotes recorded in this study are typically found growing on biofilms, such as Cryomonadida, which has  
404 already been documented in water treatment systems (Angell et al. 2020, Fried et al. 2000) and whose abundance  
405 could potentially result overestimated (Henthorne and Boysen, 2015). However, the dynamics of eukaryotic  
406 communities inside desalination plants are largely unknown and very few papers deal with this issue (e.g. Belila et al.,  
407 2017), the main focus of seawater pre-treatment studies having been bacterial biofilm eradication to prevent  
408 membrane clogging (e.g. Bar-Zeev et al., 2009). Nonetheless, due to the long period of inactivity of the Italian research  
409 station “MZS” during the winter, as well as the frequent replacement of different pre-treatment filters during most of  
410 the summer, the impact of potential biofilm growth should be minimal. As stated before, in fact, the desalination  
411 plant is also closed at the end of each expedition by pumping air in all pipes and valves, completely removing the  
412 amount of liquid seawater at the end of each expedition. This cleaning practice, together with the high amount of

413 seawater usually filtered daily through the entire desalination plant (which is fully replaced every 4 minutes) suggests  
414 as this contribution, although not quantifiable, should be really negligible. Thus, the data reported should really reflect  
415 what is present in the water column.

416 Surprisingly, diatoms, despite being usually reported as one of the main components of the phytoplanktic blooms  
417 (Pabi and Arrigo, 2006; Mangoni et al., 2009), were not abundant in our samples. Another survey, carried out during  
418 the austral summer 2011-2012, before and immediately after our sampling time frame at an offshore site, roughly 1  
419 Km far from the desalination plant intake pipe, showed a dominance of diatoms, both in terms of cell abundances and  
420 biomass, while Dinoflagellates represented only a minor group (Illuminati et al., 2017). However, the method adopted  
421 by Truzzi et al. (2015) and Illuminati et al. (2017) involved a completely different protocol based on a quali-qualitative  
422 methodology, and not based on a selective filtration process. For this reason, the absence of abundant diatom  
423 sequences in the 5  $\mu\text{m}$  “cartridge” filters may simply be due to the retention of most diatom species by the 25  $\mu\text{m}$   
424 “bag” filters located upstream. On the other hand, this apparent incongruence could also simply be due to the well-  
425 known patchy distribution of plankton communities in Terra Nova Bay, where areas dominated by diatom blooms are  
426 intermixed with others mainly dominated by dinoflagellates and other flagellates, also forming strong inshore-  
427 offshore gradients (Nuccio et al., 2000). Another reason could be related to the sub-sampling protocol and DNA  
428 extraction we have adopted. The chosen primers (Hugerth et al., 2014) should theoretically amplify 18S rRNA from  
429 Ochrophyta, as running an *in silico* PCR on the Silva SSU RefNR Database (Klindworth et al., 2013), allowing only two  
430 mismatches, reports 98% of coverage for that group. However, since the first layers of the filters were discarded and  
431 no aggressive steps, such as the mechanical lysis of diatom cell wall (frustules), were adopted during DNA extraction  
432 (Vasselon et al., 2017), it is possible that the diatom component in the total DNA extract was potentially reduced.

433 A general aspect to consider for the proposed method would also be the storage conditions for the samples which, in  
434 this case, correspond to a storage at  $-20^{\circ}\text{C}$  for some years. It is known that, despite being one of the most widespread  
435 techniques for storing samples used for molecular analyses, freezing at  $-20^{\circ}\text{C}$  could be optimal for short periods of  
436 time, whereas, on the long-term,  $-80^{\circ}\text{C}$  would be preferable (Straube and Juen, 2013). Other storage conditions were  
437 also proposed in literature, each one with different pros and cons that may condition the results of a study (e.g.  
438 Ransome et al., 2017) thus hampering comparisons between studies that adopt different storage protocols. In our  
439 case however, as samples were stored and processed under the same conditions, the comparison of observed  
440 dynamics are valid, potential biases being exactly the same for the two sets of samples.

441 An implementation of the method (which was already tested in the field during the Austral summer 2018-2019 with  
442 another set of samples) is the adoption of a subsampling procedure done immediately after filters' collection. This  
443 step greatly reduces the size of the samples (i.e. small cores instead whole filters have to be preserved) and also  
444 allows adopting different storage procedure (e.g. medium-based instead frozen). This simple step surely facilitates the  
445 storage and shipping of samples by greatly reducing their physical volume. Thanks to the increasing availability,  
446 portability and cost-efficiency of new molecular technologies (Gilbert, 2017; Johnson et al., 2017) all these analyses  
447 could also be ideally done in the field, thus completely eliminating storage-related potential issues or biases.

448

#### 449 **1.4 Conclusions:**

450 The HTS methodologies applied to the desalination plant filters, regardless of any technical peculiarity of a given  
451 desalination plant or mesh size considered, could represent a turning point in the always-increasing need of detailed  
452 and fine-scale data about the structure of phyto- and zooplankton inhabiting Antarctic coastal waters. Despite the  
453 need of further calibrations and the possible existence of issues that will require attention in the future, the  
454 availability of filters from a desalination plant offers unprecedented research opportunities at a more than achievable  
455 cost. Data shown here represent a great leap in our knowledge of coastal plankton communities for the study area,  
456 highlighting previously unknown dynamics, such as the short-term and abrupt changes in coastal nano-eukaryotic  
457 communities' composition triggered by katabatic winds pulses, and finding groups of organisms never recorded  
458 before. This approach also overcomes most of the constraints linked to the logistic of sampling activities in a harsh  
459 environment and provides precise and fine-scale data that would simply not be achievable by using standard  
460 monitoring approaches based on the collection of water samples taken in the field, e.g. from the pack-ice or a boat. By  
461 imagining a long term approach, where data of this type are collected each year at a given research station, it is out of  
462 doubts that the spatial and temporal dynamics of Antarctic coastal plankton will be revealed at unprecedented level  
463 of detail.

464

#### 465 **Acknowledgements**

466

467 We are indebted to the ENEA colleagues Francesco Pellegrino and Franco Ricci (Technical Services Leader and  
468 research Expedition Leader respectively) for their collaboration in the field and to the personnel in charge of the  
469 desalination plant during the 2011-2012, 2012-2013 and 2018-2019 field seasons, in particular Roberto Calvigioni,

470 Fabio Baglioni, Matteo Villani, for their collaboration and assistance during filter sampling procedures. We wish to  
471 thank the Ocean Biology Processing Group (OBPG) at NASA's Goddard Space Flight Center for data availability at:  
472 <https://oceancolor.gsfc.nasa.gov/>. The PNRA "Meteo-Climatological Observatory" (<http://www.climantartide.it>) has  
473 kindly allowed the use of data regarding surface air temperature and wind direction and velocity. This is a contribution  
474 of the PNRA project PNRA 16\_00120 – TNB-CODE: "Terra Nova Bay barCODing and mEtabarcoding of Antarctic  
475 organisms from marine and limno-terrestrial environments" (PI: S. Schiaparelli). This paper is also an Italian  
476 contribution to the CCAMLR CONSERVATION MEASURE 91-05 (2016) for the Ross Sea region Marine Protected Area,  
477 specifically, addressing the priorities of Annex 91-05/C, and a contribution to the SCAR-ANTOS Expert Group  
478 (<https://www.scar.org/science/antos/home/>). The authors would also like to thank three anonymous reviewers for  
479 their helpful comments that greatly improved the manuscript.

480

#### 481 **1.5 References:**

482

- 483 Angell, I.L., Bergaust, L., Hanssen, J.F., Aasen, E.M., Rudi, K., 2020. Ecological Processes Affecting Long-Term Eukaryote  
484 and Prokaryote Biofilm Persistence in Nitrogen Removal from Sewage. *Genes* (Basel). 11, 449.  
485 <https://doi.org/10.3390/genes11040449>
- 486 Baird, D.J., Hajibabaei, M., 2012. Biomonitoring 2.0: a new paradigm in ecosystem assessment made possible by next-  
487 generation DNA sequencing. *Mol. Ecol.* 21, 2039–2044. <https://doi.org/10.1111/j.1365-294X.2012.05519.x>
- 488 Balzano, S., Ellis, A. V., Le Lan, C., Leterme, S.C., 2015. Seasonal changes in phytoplankton on the north-eastern shelf of  
489 Kangaroo Island (South Australia) in 2012 and 2013. *Oceanologia* 57, 251–262.  
490 <https://doi.org/10.1016/j.oceano.2015.04.003>
- 491 Bar-Zeev, E., Berman-Frank, I., Liberman, B., Rahav, E., Passow, U., Berman, T., 2009. Transparent exopolymer  
492 particles: Potential agents for organic fouling and biofilm formation in desalination and water treatment plants.  
493 *Desalin. Water Treat.* 3, 136–142. <https://doi.org/10.5004/dwt.2009.444>
- 494 Bathmann, U., Fischer, G., Müller, P.J., Gerdes, D., 1991. Short-term variations in particulate matter sedimentation off  
495 Kapp Norvegia, Weddell Sea, Antarctica: relation to water mass advection, ice cover, plankton biomass and  
496 feeding activity. *Polar Biol.* 11, 185–195. <https://doi.org/10.1007/BF00240207>

497 Belila, A., El-Chakhtoura, J., Saikaly, P.E., van Loosdrecht, M.C.M., Vrouwenvelder, J.S., 2017. Eukaryotic community  
498 diversity and spatial variation during drinking water production (by seawater desalination) and distribution in a  
499 full-scale network. *Environ. Sci. Water Res. Technol.* 3, 92–105. <https://doi.org/10.1039/C6EW00265J>

500 Bindoff, N.L., Cheung, W.W.L., Kairo, J.G., Arstegui, J., Guinder, V.A., Hallberg, R., Hilmi, N., Jiao, N., Karim, M.S., Levin,  
501 L., 2019. Changing ocean, marine ecosystems, and dependent communities, in: IPCC Special Report on the  
502 Ocean and Cryosphere in a Changing Climate.

503 Bohmann, K., Evans, A., Gilbert, M.T.P., Carvalho, G.R., Creer, S., Knapp, M., Douglas, W.Y., De Bruyn, M., 2014.  
504 Environmental DNA for wildlife biology and biodiversity monitoring. *Trends Ecol. Evol.* 29, 358–367.  
505 <https://doi.org/10.1016/j.tree.2014.04.003>

506 Bolyen, E., Rideout, J.R., Dillon, M.R., Bokulich, N.A., Abnet, C.C., Al-Ghalith, G.A., Alexander, H., Alm, E.J., Arumugam,  
507 M., Asnicar, F., 2019. Reproducible, interactive, scalable and extensible microbiome data science using QIIME 2.  
508 *Nat. Biotechnol.* 37, 852–857. <https://doi.org/10.1038/s41587-019-0209-9>

509 Brandini, F.P., 1993. Phytoplankton biomass in an Antarctic coastal environment during stable water conditions-  
510 implications for the iron limitation theory. *Mar. Ecol. Ser.* 93, 267. <https://doi.org/10.3354/meps093267>

511 Buttigieg, P.L., Fadeev, E., Bienhold, C., Hehemann, L., Offre, P., Boetius, A., 2018. Marine microbes in 4D—using time  
512 series observation to assess the dynamics of the ocean microbiome and its links to ocean health. *Curr. Opin.*  
513 *Microbiol.* 43, 169–185. <https://doi.org/10.1016/j.mib.2018.01.015>

514 Celussi, M., Paoli, A., Crevatin, E., Bergamasco, A., Margiotta, F., Saggiomo, V., Umani, S.F., Del Negro, P., 2009. Short-  
515 term under-ice variability of prokaryotic plankton communities in coastal Antarctic waters (Cape Hallett, Ross  
516 Sea). *Estuar. Coast. Shelf Sci.* 81, 491–500. <https://doi.org/10.1016/j.ecss.2008.12.014>

517 Celussi, M., Bergamasco, A., Cataletto, B., Umani, S.F., Del Negro, P., 2010. Water masses' bacterial community  
518 structure and microbial activities in the Ross Sea, Antarctica. *Antarct. Sci.* 22, 361.  
519 <https://doi.org/10.1017/S0954102010000192>

520 Chain, F.J.J., Brown, E.A., MacIsaac, H.J., Cristescu, M.E., 2016. Metabarcoding reveals strong spatial structure and  
521 temporal turnover of zooplankton communities among marine and freshwater ports. *Divers. Distrib.* 22, 493–  
522 504. <https://doi.org/10.1111/ddi.12427>

523 Wilke, C.O., 2019. cowplot: Streamlined Plot Theme and Plot Annotations for 'ggplot2'. 2019. R package version 1.0.0.  
524 <https://CRAN.R-project.org/package=cowplot>

525 Convey, P., Peck, L.S., 2019. Antarctic environmental change and biological responses. *Sci. Adv.* 5.  
526 <https://doi.org/10.1126/sciadv.aaz0888>

527 Kelley, D., Richards, C., 2020. oce: Analysis of Oceanographic Data. R package version 1.2-0. [https://CRAN.R-](https://CRAN.R-project.org/package=oce)  
528 [project.org/package=oce](https://CRAN.R-project.org/package=oce)

529 Dayton, P.K., Kim, S., Jarrell, S.C., Oliver, J.S., Hammerstrom, K., Fisher, J.L., O'Connor, K., Barber, J.S., Robilliard, G.,  
530 Barry, J., Thurber, A.R., Conlan, K., 2013. Recruitment, Growth and Mortality of an Antarctic Hexactinellid  
531 Sponge, *Anoxycalyx joubini*. *PLoS One* 8. <https://doi.org/10.1371/journal.pone.0056939>

532 DiTullio, G.R., Grebmeier, J.M., Arrigo, K.R., Lizotte, M.P., Robinson, D.H., Leventer, A., Barry, J.P., VanWoert, M.L.,  
533 Dunbar, R.B., 2000. Rapid and early export of *Phaeocystis antarctica* blooms in the Ross Sea, Antarctica. *Nature*  
534 404, 595–598. <https://doi.org/10.1038/35007061>

535 Edgar, R.C., 2010. Search and clustering orders of magnitude faster than BLAST. *Bioinformatics* 26, 2460–2461.  
536 <https://doi.org/10.1093/bioinformatics/btq461>

537 Edgar, R.C., 2016. UNOISE2: improved error-correction for Illumina 16S and ITS amplicon sequencing. *BioRxiv* 81257.  
538 <https://doi.org/10.1101/081257>

539 Fitch, D.T., Moore, J.K., 2007. Wind speed influence on phytoplankton bloom dynamics in the Southern Ocean  
540 Marginal Ice Zone. *J. Geophys. Res. Ocean.* 112. <https://doi.org/10.1029/2006JC004061>

541 Fried, J., Mayr, G., Berger, H., Traunspurger, W., Psenner, R., Lemmer, H., 2000. Monitoring protozoa and metazoa  
542 biofilm communities for assessing wastewater quality impact and reactor up-scaling effects. *Water Sci. Technol.*  
543 41, 309–316. <https://doi.org/10.2166/wst.2000.0460>

544 Gast, R.J., Moran, D.M., Beaudoin, D.J., Blythe, J.N., Dennett, M.R., Caron, D.A., 2006. ABUNDANCE OF A NOVEL  
545 DINOFLAGELLATE PHYLOTYPE IN THE ROSS SEA, ANTARCTICA 1. *J. Phycol.* 42, 233–242.  
546 <https://doi.org/10.1111/j.1529-8817.2006.00183.x>

547 GDAL/OGR contributors, 2020. GDAL/OGR Geospatial Data Abstraction software Library. Open Source Geospatial  
548 Foundation. <https://gdal.org>

549 Gilbert, M.T.P., 2017. Documenting DNA in the dust. *Mol. Ecol.* 26, 969–971. <https://doi.org/10.1111/mec.13944>

550 Guillou, L., Bachar, D., Audic, S., Bass, D., Berney, C., Bittner, L., Boutte, C., Burgaud, G., De Vargas, C., Decelle, J., 2012.  
551 The Protist Ribosomal Reference database (PR2): a catalog of unicellular eukaryote small sub-unit rRNA  
552 sequences with curated taxonomy. *Nucleic Acids Res.* 41, D597–D604. <https://doi.org/10.1093/nar/gks1160>

553 Heimeier, D., Lavery, S., Sewell, M.A., 2010a. Molecular species identification of *Astrotooma agassizii* from planktonic  
554 embryos: further evidence for a cryptic species complex. *J. Hered.* 101, 775–779.  
555 <https://doi.org/10.1093/jhered/esq074>

556 Heimeier, D., Lavery, S., Sewell, M.A., 2010b. Using DNA barcoding and phylogenetics to identify Antarctic  
557 invertebrate larvae: Lessons from a large scale study. *Mar. Genomics* 3, 165–177.  
558 <https://doi.org/10.1016/j.margen.2010.09.004>

559 Henthorne, L., Boysen, B., 2015. State-of-the-art of reverse osmosis desalination pretreatment. *Desalination* 356, 129–  
560 139. <https://doi.org/10.1016/j.desal.2014.10.039>

561 Herlemann, D.P.R., Labrenz, M., Jürgens, K., Bertilsson, S., Waniek, J.J., Andersson, A.F., 2011. Transitions in bacterial  
562 communities along the 2000 km salinity gradient of the Baltic Sea. *ISME J.* 5, 1571–1579.  
563 <https://doi.org/10.1038/ismej.2011.41>

564 Hugerth, L.W., Muller, E.E.L., Hu, Y.O.O., Lebrun, L.A.M., Roume, H., Lundin, D., Wilmes, P., Andersson, A.F., 2014.  
565 Systematic design of 18S rRNA gene primers for determining eukaryotic diversity in microbial consortia. *PLoS*  
566 *One* 9, e95567. <https://doi.org/10.1371/journal.pone.0095567>

567 Illuminati, S., Annibaldi, A., Romagnoli, T., Libani, G., Antonucci, M., Scarponi, G., Totti, C., Truzzi, C., 2017. Distribution  
568 of Cd, Pb and Cu between dissolved fraction, inorganic particulate and phytoplankton in seawater of Terra  
569 Nova Bay (Ross Sea, Antarctica) during austral summer 2011–12. *Chemosphere* 185, 1122–1135.  
570 <https://doi.org/10.1016/j.chemosphere.2017.07.087>

571 Johnson, S.S., Zaikova, E., Goerlitz, D.S., Bai, Y., Tighe, S.W., 2017. Real-time DNA sequencing in the Antarctic dry  
572 valleys using the Oxford Nanopore sequencer. *J. Biomol. Tech.* JBT 28, 2. [https://doi.org/10.7171/jbt.17-2801-](https://doi.org/10.7171/jbt.17-2801-009)  
573 [009](https://doi.org/10.7171/jbt.17-2801-009)

574 Jovel, J., Patterson, J., Wang, W., Hotte, N., O’Keefe, S., Mitchel, T., Perry, T., Kao, D., Mason, A.L., Madsen, K.L., 2016.  
575 Characterization of the gut microbiome using 16S or shotgun metagenomics. *Front. Microbiol.* 7, 459.  
576 <https://doi.org/10.3389/fmicb.2016.00459>

577 Kanta, M.R., Babula, J., Anilkumar, N.P., Krishna, N.R., Bhaskar, P.V., Soares, M.A., 2017. Variability of chlorophyll-a  
578 and diatoms in the frontal ecosystem of Indian Ocean sector of the Southern Ocean. *Polish Polar Res.* 375–392.  
579 <https://doi.org/10.1515/popore-2017-0014>



580 Klindworth, A., Pruesse, E., Schweer, T., Peplies, J., Quast, C., Horn, M., Glöckner, F.O., 2013. Evaluation of general 16S  
581 ribosomal RNA gene PCR primers for classical and next-generation sequencing-based diversity studies. *Nucleic  
582 Acids Res.* 41, e1–e1. <https://doi.org/10.1093/nar/gks808>

583 Lacoursière-Roussel, A., Howland, K., Normandeau, E., Grey, E.K., Archambault, P., Deiner, K., Lodge, D.M., Hernandez,  
584 C., Leduc, N., Bernatchez, L., 2018. eDNA metabarcoding as a new surveillance approach for coastal Arctic  
585 biodiversity. *Ecol. Evol.* 8, 7763–7777. <https://doi.org/10.1002/ece3.4213>

586 Liu, Q., Zhao, Q., McMinn, A., Yang, E.J., Jiang, Y., 2020. Planktonic microbial eukaryotes in polar surface waters:  
587 recent advances in high-throughput sequencing. *Mar. Life Sci. Technol.* 1–9. [https://doi.org/10.1007/s42995-  
588 020-00062-y](https://doi.org/10.1007/s42995-020-00062-y)

589 Lo Giudice, A., Caruso, C., Mangano, S., Bruni, V., De Domenico, M., Michaud, L., 2012. Marine bacterioplankton  
590 diversity and community composition in an Antarctic coastal environment. *Microb. Ecol.* 63, 210–223.  
591 <https://doi.org/10.1007/s00248-011-9904-x>

592 Lo Giudice, A., Azzaro, M., 2019. Diversity and ecological roles of prokaryotes in the changing Antarctic marine  
593 environment, in: *The Ecological Role of Micro-Organisms in the Antarctic Environment*. Springer, pp. 109–131.

594 Love, M.I., Huber, W., Anders, S., 2014. Moderated estimation of fold change and dispersion for RNA-seq data with  
595 DESeq2. *Genome Biol.* 15, 550. <https://doi.org/10.1186/s13059-014-0550-8>

596 Lynn, D., 2008. *The ciliated protozoa: characterization, classification, and guide to the literature*. Springer Science &  
597 Business Media.

598 Mangoni, O., Saggiomo, M., Modigh, M., Catalano, G., Zingone, A., Saggiomo, V., 2009. The role of platelet ice  
599 microalgae in seeding phytoplankton blooms in Terra Nova Bay (Ross Sea, Antarctica): a mesocosm experiment.  
600 *Polar Biol.* 32, 311–323. <https://doi.org/10.1007/s00300-008-0507-z>

601 Martin, M., 2011. Cutadapt removes adapter sequences from high-throughput sequencing reads. *EMBnet. J.* 17, 10–  
602 12. <https://doi.org/10.14806/ej.17.1.200>

603 Matsuoka, K., Skoglund, A., Roth, G., 2018. *Quantarctica*, Norwegian Polar Institute.  
604 <https://www.npolar.no/quantarctica/>

605 McMurdie, P.J., Holmes, S., 2013. phyloseq: an R package for reproducible interactive analysis and graphics of  
606 microbiome census data. *PLoS One* 8, e61217. <https://doi.org/10.1371/journal.pone.0061217>

607 McMurdie, P.J., Holmes, S., 2014. Waste not, want not: why rarefying microbiome data is inadmissible. *PLoS Comput  
608 Biol* 10, e1003531. <https://doi.org/10.1371/journal.pcbi.1003531>

609 Moline, M.A., Prezelin, B.B., 1996. Long-term monitoring and analyses of physical factors regulating variability in  
610 coastal Antarctic phytoplankton biomass, in situ productivity and taxonomic composition over subseasonal,  
611 seasonal and interannual time scales. *Mar. Ecol. Prog. Ser.* 145, 143–160. <https://doi.org/10.3354/meps145143>

612 Monti, M., Zoccarato, L., Umani, S.F., 2017. Microzooplankton composition under the sea ice and in the open waters  
613 in Terra Nova Bay (Antarctica). *Polar Biol.* 40, 891–901. <https://doi.org/10.1007/s00300-016-2016-9>

614 Moreira, D., López-García, P., 2019. Time series are critical to understand microbial plankton diversity and ecology.  
615 *Mol. Ecol.* 28, 920–922. <https://doi.org/10.1111/mec.15015>

616 NASA Goddard Space Flight Center, Ocean Ecology Laboratory, Ocean Biology Processing Group, 2018a. Moderate-  
617 resolution Imaging Spectroradiometer (MODIS) Aqua Chlorophyll Data Reprocessing. NASA OB.DAAC,  
618 Greenbelt, MD, USA. <https://oceancolor.gsfc.nasa.gov/data/10.5067/AQUA/MODIS/L3M/CHL/2018/> (accessed  
619 12 November 2019)

620 NASA Goddard Space Flight Center, Ocean Ecology Laboratory, Ocean Biology Processing Group, 2018b. Moderate-  
621 resolution Imaging Spectroradiometer (MODIS) Aqua Particulate Organic Carbon Data Reprocessing. NASA  
622 OB.DAAC, Greenbelt, MD, USA. [https://oceancolor.gsfc.nasa.gov/data/10.5067/AQUA/MODIS/L3M/POC/2018](https://oceancolor.gsfc.nasa.gov/data/10.5067/AQUA/MODIS/L3M/POC/2018/)  
623 (accessed 12 November 2019)

624 Navarro, L.M., Fernández, N., Guerra, C., Guralnick, R., Kissling, W.D., Londoño, M.C., Muller-Karger, F., Turak, E.,  
625 Balvanera, P., Costello, M.J., 2017. Monitoring biodiversity change through effective global coordination. *Curr.*  
626 *Opin. Environ. Sustain.* 29, 158–169. <https://doi.org/10.1016/j.cosust.2018.02.005>

627 Nieblas, A.-E., Sloyan, B.M., Hobday, A.J., Coleman, R., Richardsone, A.J., 2009. Variability of biological production in  
628 low wind-forced regional upwelling systems: A case study off southeastern Australia. *Limnol. Oceanogr.* 54,  
629 1548–1558. <https://doi.org/10.4319/lo.2009.54.5.1548>

630 Nuccio, C., Innamorati, M., Lazzara, L., Mori, G., Massi, L., 2000. Spatial and temporal distribution of phytoplankton  
631 assemblages in the Ross Sea, in: *Ross Sea Ecology*. Springer, pp. 231–245. [https://doi.org/10.1007/978-3-642-  
632 59607-0\\_19](https://doi.org/10.1007/978-3-642-59607-0_19)

633 Pabi, S., Arrigo, K.R., 2006. Satellite estimation of marine particulate organic carbon in waters dominated by different  
634 phytoplankton taxa. *J. Geophys. Res. Ocean.* 111. <https://doi.org/10.1029/2005JC003137>

635 Park, J., Kim, J., Kim, H., Hwang, J., Jo, Y., Lee, S.H., 2019. Environmental forcings on the remotely sensed  
636 phytoplankton bloom phenology in the central Ross Sea Polynya. *J. Geophys. Res. Ocean.* 124, 5400–5417.  
637 <https://doi.org/10.1029/2019JC015222>

638 Piñol, J., Senar, M.A., Symondson, W.O.C., 2019. The choice of universal primers and the characteristics of the species  
639 mixture determine when DNA metabarcoding can be quantitative. *Mol. Ecol.* 28, 407–419.  
640 <https://doi.org/10.1111/mec.14776>

641 Proença, V., Martin, L.J., Pereira, H.M., Fernandez, M., McRae, L., Belnap, J., Böhm, M., Brummitt, N., García-Moreno,  
642 J., Gregory, R.D., 2017. Global biodiversity monitoring: from data sources to essential biodiversity variables.  
643 *Biol. Conserv.* 213, 256–263. <https://doi.org/10.1016/j.biocon.2016.07.014>

644 QGIS Development Team, 2020. QGIS Geographic Information System. Open Source Geospatial Foundation Project.  
645 <http://qgis.osgeo.org>

646 Qu, B., Gabric, A.J., Zeng, M., Liu, X., 2020. Correlations among phytoplankton biomass, sea ice and wind speed in  
647 Barents Sea and the future climate trends. *Polar Sci.* 100525. <https://doi.org/10.1016/j.polar.2020.100525>

648 Quast, C., Pruesse, E., Yilmaz, P., Gerken, J., Schweer, T., Yarza, P., Peplies, J., Glöckner, F.O., 2012. The SILVA  
649 ribosomal RNA gene database project: improved data processing and web-based tools. *Nucleic Acids Res.* 41,  
650 D590–D596. <https://doi.org/10.1093/nar/gks1219>

651 R Core Team, 2020. R: A language and environment for statistical computing. R Foundation for Statistical Computing,  
652 Vienna, Austria. <https://www.R-project.org>

653 Rajaram, S., Oono, Y., 2010. NeatMap-non-clustering heat map alternatives in R. *BMC Bioinformatics* 11, 1–9.  
654 <https://doi.org/10.1186/1471-2105-11-45>

655 Ransome, E., Geller, J.B., Timmers, M., Leray, M., Mahardini, A., Sembiring, A., Collins, A.G., Meyer, C.P., 2017. The  
656 importance of standardization for biodiversity comparisons: A case study using autonomous reef monitoring  
657 structures (ARMS) and metabarcoding to measure cryptic diversity on Mo’orea coral reefs, French Polynesia.  
658 *PLoS One* 12, e0175066. <https://doi.org/10.1371/journal.pone.0175066>

659 Rognes, T., Flouri, T., Nichols, B., Quince, C., Mahé, F., 2016. VSEARCH: a versatile open source tool for metagenomics.  
660 *PeerJ* 4, e2584. <https://doi.org/10.7717/peerj.2584>

661 Saggiomo, M., Poulin, M., Mangoni, O., Lazzara, L., De Stefano, M., Sarno, D., Zingone, A., 2017. Spring-time dynamics  
662 of diatom communities in landfast and underlying platelet ice in Terra Nova Bay, Ross Sea, Antarctica. *J. Mar.*  
663 *Syst.* 166, 26–36. <https://doi.org/10.1016/j.jmarsys.2016.06.007>

664 Sallée, J.-B., Llorc, J., Tagliabue, A., Lévy, M., 2015. Characterization of distinct bloom phenology regimes in the  
665 Southern Ocean. *ICES J. Mar. Sci.* 72, 1985–1998. <https://doi.org/10.1093/icesjms/fsv069>

666 Sazhin, A.F., Artigas, L.F., Nejstgaard, J.C., Frischer, M.E., 2007. The colonization of two *Phaeocystis* species  
667 (*Prymnesiophyceae*) by pennate diatoms and other protists: a significant contribution to colony biomass, in:  
668 *Phaeocystis*, Major Link in the Biogeochemical Cycling of Climate-Relevant Elements. Springer, pp. 137–145.  
669 <https://doi.org/10.1007/s10533-007-9086-2>

670 Schloss, P.D., Westcott, S.L., Ryabin, T., Hall, J.R., Hartmann, M., Hollister, E.B., Lesniewski, R.A., Oakley, B.B., Parks,  
671 D.H., Robinson, C.J., 2009. Introducing mothur: open-source, platform-independent, community-supported  
672 software for describing and comparing microbial communities. *Appl. Environ. Microbiol.* 75, 7537–7541.  
673 <https://doi.org/10.1128/AEM.01541-09>

674 Sewell, M., Lavery, S., Baker, C., 2006. Whose larva is that? Molecular identification of planktonic larvae of the Ross  
675 Sea. *New Zeal. Aquat. Environ. Biodivers. Rep.* <https://researchspace.auckland.ac.nz/handle/2292/8452>

676 Sewell, M.A., Jury, J.A., 2009. Desalination plants as plankton sampling devices in temporal studies: proof-of-concept  
677 and suggestions for the future. *Limnol. Oceanogr. Methods* 7, 363–370.  
678 <https://doi.org/10.4319/lom.2009.7.363>

679 Sewell, M.A., Jury, J.A., 2011. Seasonal patterns in diversity and abundance of the High Antarctic meroplankton:  
680 plankton sampling using a Ross Sea desalination plant. *Limnol. Oceanogr.* 56, 1667–1681.  
681 <https://doi.org/10.4319/lo.2011.56.5.1667>

682 Signal developers, 2014. signal: Signal processing. <http://r-forge.r-project.org/projects/signal/>

683 Smith Jr, W.O., Dennett, M.R., Mathot, S., Caron, D.A., 2003. The temporal dynamics of the flagellated and colonial  
684 stages of *Phaeocystis antarctica* in the Ross Sea. *Deep Sea Res. Part II Top. Stud. Oceanogr.* 50, 605–617.  
685 [https://doi.org/10.1016/S0967-0645\(02\)00586-6](https://doi.org/10.1016/S0967-0645(02)00586-6)

686 Straube, D., Juen, A., 2013. Storage and shipping of tissue samples for DNA analyses: A case study on earthworms. *Eur.*  
687 *J. Soil Biol.* 57, 13–18. <https://doi.org/10.1016/j.ejsobi.2013.04.001>

688 Taberlet, P., Coissac, E., Pompanon, F., Brochmann, C., Willerslev, E., 2012. Towards next-generation biodiversity  
689 assessment using DNA metabarcoding. *Mol. Ecol.* 21, 2045–2050. [https://doi.org/10.1111/j.1365-](https://doi.org/10.1111/j.1365-294X.2012.05470.x)  
690 [294X.2012.05470.x](https://doi.org/10.1111/j.1365-294X.2012.05470.x)

691 Taberlet, P., Bonin, A., Coissac, E., Zinger, L., 2018. Environmental DNA: For biodiversity research and monitoring.  
692 Oxford University Press. <https://doi.org/10.1093/oso/9780198767220.001.0001>

693 Torstensson, A., Dinasquet, J., Chierici, M., Fransson, A., Riemann, L., Wulff, A., 2015. Physicochemical control of  
694 bacterial and protist community composition and diversity in Antarctic sea ice. *Environ. Microbiol.* 17, 3869–  
695 3881. <https://doi.org/10.1111/1462-2920.12865>

696 Tripathy, S.C., Jena, B., 2019. Iron-Stimulated Phytoplankton Blooms in the Southern Ocean: a Brief Review. *Remote*  
697 *Sens. Earth Syst. Sci.* 2, 64–77. <https://doi.org/10.1007/s41976-019-00012-y>

698 Truzzi, C., Annibaldi, A., Finale, C., Libani, G., Romagnoli, T., Scarponi, G., Illuminati, S., 2015. Separation of micro-  
699 phytoplankton from inorganic particulate in Antarctic seawater (Ross Sea) for the determination of Cd, Pb and  
700 Cu: optimization of the analytical methodology. *Anal. Methods* 7, 5490–5496.  
701 <https://doi.org/10.1039/C5AY00730E>

702 Valentini, A., Taberlet, P., Miaud, C., Civade, R., Herder, J., Thomsen, P.F., Bellemain, E., Besnard, A., Coissac, E., Boyer,  
703 F., 2016. Next-generation monitoring of aquatic biodiversity using environmental DNA metabarcoding. *Mol.*  
704 *Ecol.* 25, 929–942. <https://doi.org/10.1111/mec.13428>

705 Vasselon, V., Domaizon, I., Rimet, F., Kahlert, M., Bouchez, A., 2017. Application of high-throughput sequencing (HTS)  
706 metabarcoding to diatom biomonitoring: Do DNA extraction methods matter? *Freshw. Sci.* 36, 162–177.  
707 <https://doi.org/10.1086/690649>

708 Veerapaneni, S., Long, B., Freeman, S., Bond, R., 2007. Reducing energy consumption for seawater desalination.  
709 *Journal-American Water Work. Assoc.* 99, 95–106. <https://doi.org/10.1002/j.1551-8833.2007.tb07958.x>

710 Villacorte, L.O., Tabatabai, S.A.A., Anderson, D.M., Amy, G.L., Schippers, J.C., Kennedy, M.D., 2015. Seawater reverse  
711 osmosis desalination and (harmful) algal blooms. *Desalination* 360, 61–80.  
712 <https://doi.org/10.1016/j.desal.2015.01.007>

713 Wang, E., Cook, D., Hyndman, R.J., 2020. A new tidy data structure to support exploration and modeling of temporal  
714 data. *J. Comput. Graph. Stat.* 1–13. <https://doi.org/10.1080/10618600.2019.1695624>

715 Wang, Q., Garrity, G.M., Tiedje, J.M., Cole, J.R., 2007. Naive Bayesian classifier for rapid assignment of rRNA sequences  
716 into the new bacterial taxonomy. *Appl. Environ. Microbiol.* 73, 5261–5267.  
717 <https://doi.org/10.1128/AEM.00062-07>

718 West, K.M., Stat, M., Harvey, E.S., Skepper, C.L., DiBattista, J.D., Richards, Z.T., Travers, M.J., Newman, S.J., Bunce, M.,  
719 2020. eDNA metabarcoding survey reveals fine-scale coral reef community variation across a remote, tropical  
720 island ecosystem. *Mol. Ecol.* 29, 1069–1086. <https://doi.org/10.1111/mec.15382>

721 Wickham, H., Francois, R., Henry, L., Müller, K., 2020. Package dplyr: A Grammar of Data Manipulation. R package  
722 version 0.8.5. <https://CRAN.R-project.org/package=dplyr>

723 Wickham, H., 2016. ggplot2: Elegant Graphics for Data Analysis. Springer-Verlag New York.  
724 <https://ggplot2.tidyverse.org>

725 Wilkins, D., Yau, S., Williams, T.J., Allen, M.A., Brown, M. V, DeMaere, M.Z., Lauro, F.M., Cavicchioli, R., 2013. Key  
726 microbial drivers in Antarctic aquatic environments. *FEMS Microbiol. Rev.* 37, 303–335.  
727 <https://doi.org/10.1111/1574-6976.12007>

728 Wolf, P.H., Siverns, S., Monti, S., 2005. UF membranes for RO desalination pretreatment. *Desalination* 182, 293–300.  
729 <https://doi.org/10.1016/j.desal.2005.05.006>

730 Zhang, G.K., Chain, F.J.J., Abbott, C.L., Cristescu, M.E., 2018. Metabarcoding using multiplexed markers increases  
731 species detection in complex zooplankton communities. *Evol. Appl.* 11, 1901–1914.  
732 <https://doi.org/10.1111/eva.12694>

733 Zoccarato, L., Pallavicini, A., Cerino, F., Umani, S.F., Celussi, M., 2016. Water mass dynamics shape Ross Sea protist  
734 communities in mesopelagic and bathypelagic layers. *Prog. Oceanogr.* 149, 16–26.  
735 <https://doi.org/10.1016/j.pocean.2016.10.003>

736

737

738

739

740

741

742

743

744

745

746

747

748

749 **Figure Captions:**

750 Fig. 1. Overview on Gerlache Inlet (Terra Nova Bay, TNB) showing the three research stations operating in TNB: Mario  
751 Zucchelli Station (IT=Italy), Gondwana Station (DE=Germany) and Jang Bogo Station (KR=Republic of Korea).  
752 The red squares indicate the research stations operating only during the summer, whereas the red and blue  
753 square indicate the only all year-round operating research station (Jang Bogo). The map was produced using  
754 the collection of datasets “Quantarctica” (Matsuoka et al., 2018) and the 2.18 version of QGIS (QGIS  
755 Development Team, 2020). The map depicts the coastline orientation before the desalination plant seawater  
756 intake pipe (red arrow) in the locality of Punta Stocchino and of the Automatic Weather Station (AWS) “Eneide”  
757 (yellow circle).

758 Fig. 2. Desalination plant of Mario Zucchelli station. (a) View of the plant pump shed in the locality of Punta Stocchino.  
759 (b) 25  $\mu\text{m}$  (left) and 5  $\mu\text{m}$  (right) filter housings in the desalination plant powerhouse. (c) New cartridge filters  
760 (5  $\mu\text{m}$ ) just replaced before the closure of the lid of the filter housing.

761 Fig. 3. Simplified diagram of MZS desalination plant.

762 Fig. 4. (a) A frozen cartridge filter sampled on February 4th after having filtered  $\sim 22.5$  hours. The three replicates were  
763 sampled from both extremities and the centre (blue arrows). (b) Layers of polypropylene extracted using a cork  
764 borer and a pair of heat-sterilized tweezers prior to the DNA extraction. Successively, the layers were cut in half  
765 and then in stripes of 1 mm of width.

766 Fig. 5. Boxplots of log-diary and satellite data from 2002 to 2019. Upper boxplots refer to (a) filter activity hours for  
767 bag filters (25  $\mu\text{m}$  mesh size) and (b) cartridge filters (5  $\mu\text{m}$  mesh size). Boxplots in the middle refer to (c)  
768 Particulate Organic Carbon (POC) and (d) Chlorophyll concentration measured in milligrams per cubic meter.  
769 Lower boxplot (e) refers to the total monthly cubic meters of water consumed by the research station. All data  
770 has been gathered based on month of registration and ordered from October to February. Satellite data for  
771 Chlorophyll and POC in October are less abundant than for the other months, as most of the area is usually  
772 covered in sea-ice during that period. Filters were assigned to month on the base of their installation time.

773 Fig. 6. Non-metric Multidimensional Scaling of 16S and 18S based on Bray-Curtis distances. Colours refer to the  
774 replicates of the same filter, thus corresponding to the same day of sampling. Dates in the legend are ordered  
775 in temporal succession. Triangles refer to 2012 samples and circles to 2013 samples.

776 Fig. 7. Scatterplot showing the correlation between the two different matrices of Bray-Curtis distances for 18S and  
777 16S.

778 Fig. 8. (a) Taxa barplots for 18S of 2012 (left) and 2013 (right). (b) Taxa barplots for 16S of 2012 (left) and 2013 (right).

779 Fig. 9. Barplots of hourly wind speed recordings (a,b) and wind roses (c,d) for the two different time ranges  
780 investigated during 2012 and 2013. (a) The wind intensity (knots) and c) wind rose at the bottom for the 2012  
781 series, (b) and (d) for the 2013 series. Blue and green bands below the barplots indicate activity time ranges for  
782 the individual filters sampled for this study, whereas the grey areas represent the activity time of filters that  
783 couldn't be sampled for this study.

784 Fig. 10. Heatmap of 18S 50 most abundant ZOTUs (left) and 16S 1,000 most abundant ZOTUs (right), the latter  
785 agglomerated by taxonomic order (fourth level from the highest of the Silva database taxonomy). Abundances  
786 values refer to those given after the variance stabilizing transformation. The x-axis is sorted in chronological  
787 order, from the oldest to the most recent filter, with the 2012 series on the left and the 2013 on the right, for  
788 both heatmaps.



Desalination  
plant cartridge filters  
(5  $\mu\text{m}$  mesh size)

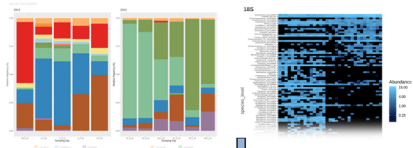


nanoplankton collection

Metabarcoding



Intra- and inter-annual dynamics



Link to environmental drivers

